University of Leoben

Modeling Massive Hydraulic Fractures in Full-Field Reservoir Simulation

Diploma Thesis

Astrid Wernisch

Leoben, 9th of October 2008

Affidavit:

I declare in lieu of oath, that I wrote this thesis and performed the associated research myself, using only literature cited in this volume.

_____

Astrid Wernisch

Leoben, 9th of October 2008

Acknowledgements

My sincerest gratitude is to Dr. Leonhard Ganzer, for his great patience, understanding, help and valuable hints throughout the development of this diploma thesis.

I want to express my gratitude to HOT Engineering, for giving me the opportunity to write about the topic of “Modeling massive hydraulic fractures in full-field reservoir simulation”, and especially to Dipl.-Ing. Reinhard Lind for his support and helpful hints.

Thanks to Dipl.-Ing. Barbara Pirker for her scientific and technical help and much needed motivation.

In equal measure, I want to thank Matthias Buchebner for his technical support in the big, wide world of computer programming and data processing.

I would like to give my special thanks to Richard Rachbauer for reviewing the manuscript, for his constant ideas of improvement and a smile at the right time.

At last, I am deeply indebted to my family, who helped and supported me in all the time of my studies.

Table of contents

List of figures

List of tables

Kurzfassung

Hydraulisches Zerklüften ist eines der primären Werkzeuge um die Produktivität eines Bohrlochs zu steigern. Das Stimulieren des Bohrlochs durch solch eine Behandlung führt üblicherweise zu einem negativen Skin Faktor. Ziel dieser Arbeit ist es, Probleme mit negativen Skin Faktoren zu beschreiben und ein bereits vorhandenes Lagerstättenmodel so zu verändern, dass keine Schwierigkeiten aufgrund von einem negativen Skin Faktor auftreten. Das Überschreiten eines bestimmten Grenzwertes führt zu einem Absturz der Simulation. Der Skin Faktor wird durch die Geometrie und Permeabilität des Gitterblocks definiert, in dem sich das stimulierte Bohrloch befindet. Die explizite Diskretisierung von hydraulisch erzeugten Klüften in einem Lagerstättenmodell ist zeit- und kostenaufwendig. Diese Arbeit zielt auf eine Methode ab, einen hohen negativen Skin Faktor in einem kommerziellen Lagerstättensimulator zu handhaben.

Mit dem Konzept des effektiven Bohrlochradius und dem druck-äquivalenten Radius sind zwei Ansätze zur Berechnung des Skin Faktor Grenzwertes gegeben. Ein paar Überlegungen zum Umgehen eines hohen negativen Skin Faktors werden dargestellt. Der Verbindungs-Transmissibilitäts-Multiplikator liefert das zuverlässigste Ergebnis. Dieser wird anstatt eines Skin Faktors in die Simulationsdatei inkludiert. Neben der Anwendung in einem Gasinjektionsbohrloch wird die Zuverlässigkeit dieses Multiplikators in verschiedenen Beispielen, unter anderem einem horizontalem Bohrloch, getestet.

Abstract

Hydraulic fracturing is one of the primary engineering tools to increase the productivity of a well. Stimulating a well by a hydraulic fracturing treatment usually leads to a high negative skin factor. This work aims to define the problem and to modify an existing reservoir simulation model, such that negative skin factors do not cause constant difficulties. Changing the negative skin factor in the simulation model below a threshold value leads to an abnormal end of the simulation run. The skin factor is defined by the geometry and the permeability of the grid block containing the now stimulated well. As the explicit discretization of hydraulic fractures in the reservoir model is time- and cost intensive, this thesis focuses on a method to handle a high negative skin factor in a commercial reservoir simulator.

With the concepts of the effective wellbore radius and the pressure equivalent radius two approaches to calculate the threshold skin factor are given. Some considerations are demonstrated to avoid the use of a negative skin factor. The most accurate result is delivered by the connection transmissibility multiplier, which is included in the simulation file instead of a negative skin factor. Besides the application in a vertical gas injection well the precision of this multiplier is represented in multiple application examples, including changed geometry and permeability properties. Finally, the utilization of the multiplier in horizontal wells is also discussed.

Introduction

During the last decade, the worldwide demand for oil increased drastically. Simultaneously, the development of the oil price increased up to ~100 US $ per barrel[1]. Nowadays, less and less promising hydrocarbon reservoirs are explored, therefore secondary and tertiary oil recovery techniques become more and more economic. Especially operators of weaker, often damaged and uneconomic wells are interested to enhance the production by application of these techniques.

The fundamental tool in petroleum industry to optimize the development of a reservoir is reservoir stimulation. The main objective of well stimulation is to enhance the productivity of a well by improving the fluid flow from the reservoir into the wellbore. Different stimulation techniques, like hydraulic fracturing, fracpack, carbonate and sandstone matrix acidizing are used in oil industry [1].

In general a stimulation treatment reduces the permeability in the vicinity of a well and enlarges the flow channels which connect the formation with the wellbore. As an efficiency indicator for these treatments the skin factor can be used. An increased productivity after well stimulation results in a decreasing, and often even negative, skin factor. Hydraulic fracturing turned out to be the most efficient method to increase the productivity and therefore to reach the most negative skin factors of old and damaged wells.

Nowadays, for most of the production wells a reservoir simulation model already exists. Due to a stimulation job, the properties of the now stimulated well do not correspond to the properties of the well in the existing model. Creating a new reservoir model, which takes the hydraulic fractures into account, is fairly time- and cost-consuming. Thus, the possibility of implementing the altered properties in the existing model has to be considered as an interesting alternative. Unfortunately, the implementation of the high negative skin factor often causes problems in commercial simulation software.

Hence, the challenge of this thesis is to define the apparent problems in the simulation software. Moreover a modification of an existing reservoir simulation model will be performed, such that the negative skin factors will not cause constant difficulties during simulation.

[1] from www.handelsblatt.com/rohstoffe-devisen/Oel-Preis, 09/12/2008, Brent Oil 97.81 US $

In this thesis basically the application of different skin factors and multipliers is tested in a vertical gas injection well. Multiple application examples represent the precision of the calculated multipliers for changed geometry and permeability properties. At last the utilization of the multipliers in a horizontal well is tested.

For the simulation part the ECLIPSE 100 simulation software, Version 2007.2., from Schlumberger is utilized [2, 3].

1 Hydraulic fracturing

Hydraulic fracturing is a well-stimulation technique and may be defined as the process of injecting fluid in a porous medium with such pressure that a fracture or a fracture system is created. When rock is put under tension only little or no plastic deformation takes place, and the formation breaks at the yield point. If fluid is pumped into a well faster than the fluid can escape into the surrounding formation, the pressure in the wellbore increases to a value that exceeds the breakdown pressure of the formation open to the wellbore.

A fracture is created that spreads in two directions from the wellbore as a result of tensile hoop stresses generated by the internal pressure. The generated fracture continues to propagate and grows as long as the injected fluid moves down the fracture and increases the formation area. Once pumping stops and the injected fluid leaks off, the fracture will close and the new formation area will not be available for production [1, 4-9].

To prevent the closing of the fractures, a so called propping agent must be added to the fluid and transported to the fracture. The purpose of this propping agent (called the “pad”) is to hold the fracture open once the pumps are shut down and permit the fluid to flow. For ideal results the pad requires being strong, resistant to crushing and corrosion, and should be readily available at low cost. Usually, these propping agents are silica sand, resin-coated sand, and ceramic proppants [1, 4, 8].

1.1 Objectives of fracturing

In general, hydraulic fracture treatments are performed on a well to enhance the productivity index or the injectivity index. The productivity index defines the relationship between the production rate of oil or gas and the pressure drawdown between the wellbore and the reservoir. Contrary, the injectivity index relates to the relationship between the injection rate at which a fluid can be injected into a well at a given pressure differential between the wellbore and the reservoir [8].

- ✓ Bypass near-wellbore damage:

Near-wellbore damage results in a reduction of the permeability and therefore in reducing the well productivity. The reasons for this damage are basically the invasion of

drilling fluid into the reservoir while drilling, where the pores and pore throats are plugged by mud solids, and the invasion of cement during casing and cementing jobs. Also the chemical incompatibility between the drilling fluids and the formation is a source of damage. Furthermore, natural processes alter the reservoir rock over time, such as diagenetic processes, which restrict the openings in the rock, changes in saturation due to low reservoir pressure near the wellbore, formation fines movement or scale deposition. The depth of the damage depends on the near-wellbore conditions, the rock properties and the properties of the mud filtrate and solids.

Often, such wells are uneconomical unless a high-conductivity path is produced by a hydraulic fracture treatment. This conductivity path connects the wellbore with the undamaged rock and returns the well to its natural productivity [1, 8].

- ✓ Increase productivity:

Related to Darcy's law (Eq.1) hydraulic fracturing can improve the productivity of a well by increasing the formation flow area (enlarging the flow channels).

$$q = \frac{kh}{\mu}\frac{\Delta p}{\Delta x}\left(\frac{A}{h}\right) \quad \text{.....(1)}$$

The treatment can expand a conductivity path deep into the reservoir, enhance the productivity beyond the natural level and increase the present value for the reserves. In general a stimulation job can increase the productivity of a well by 200 to 500 percent. The effective production increase is affected by the length, height, and width of the produced fracture, influencing the absorption of fluids from the formation. The transport of the fluid to the wellbore depends on the fracture permeability [1, 4, 7].

- ✓ Alter fluid flow:

Beside the improvement of well productivity, hydraulic fracturing is also a potent resource for altering the fluid flow in the reservoir. The high pressure drawdown at the near wellbore zone may cause water or gas coning into the wellbore. Fracture treatment can decrease the pressure drop around the well and minimize water or gas coning, sand production and problems with asphaltine and paraffin deposition. Enhanced gravel-packing sand placement and optimized reserve recovery are also possible. By knowing the geometry and direction of the fracture the sweep efficiency can also be improved and

this results in a more efficient field development. Fracture design has an influence in planning other wells and is therefore a powerful tool for reservoir management [1, 4, 8].

1.2 Candidate selection

As the fracturing treatment increases the production rate of a well, the potential reservoir must contain enough fluids in place and must be able to move the fluids through the high-conductive channels. In general, such reservoirs exhibit a thick pay zone, medium to high pressure and low to moderate permeability. Also a stress-barrier is needed, in order to limit the vertical growth of a fracture. Damaged wells are also good candidates for hydraulic fracturing.

Contrary, reservoirs with thin pay zone, low reservoir pressure, and a small areal extent are poor candidates for a stimulation treatment. Extremely low permeability reservoirs may not be efficient enough to pay all the operational cost, even if stimulated successfully [8].

The most important parameters in candidate selection are reservoir pressure, permeability, in-situ stress distribution, skin factor and the conditions at the wellbore. Before a well is selected for a fracturing job, several criteria have to be considered.

- If the well has additional gas or oil to produce
- If the well has sufficient reservoir pressure to move the fluid to the fracture
- If the well has been damaged during drilling and completion operations
- If there is enough reservoir pressure in old pumping wells
- If the formation already contains natural fracture networks
- If the well is a production or an injection well
- If there is a deposition of fines, scales, wax or paraffin
- If the well is vertical or horizontal

1.3 Fracture mechanics

Rock and fluid mechanics considerations control the created fracture geometry and the fracture dimensions. Reservoir formations are subjected to a stress field that can be divided into three principal stresses. Figure 1 illustrates this stress field, where σ_v is the vertical stress, σ_{Hmin} is the minimum horizontal stress, and σ_{Hmax} is the maximum horizontal stress.

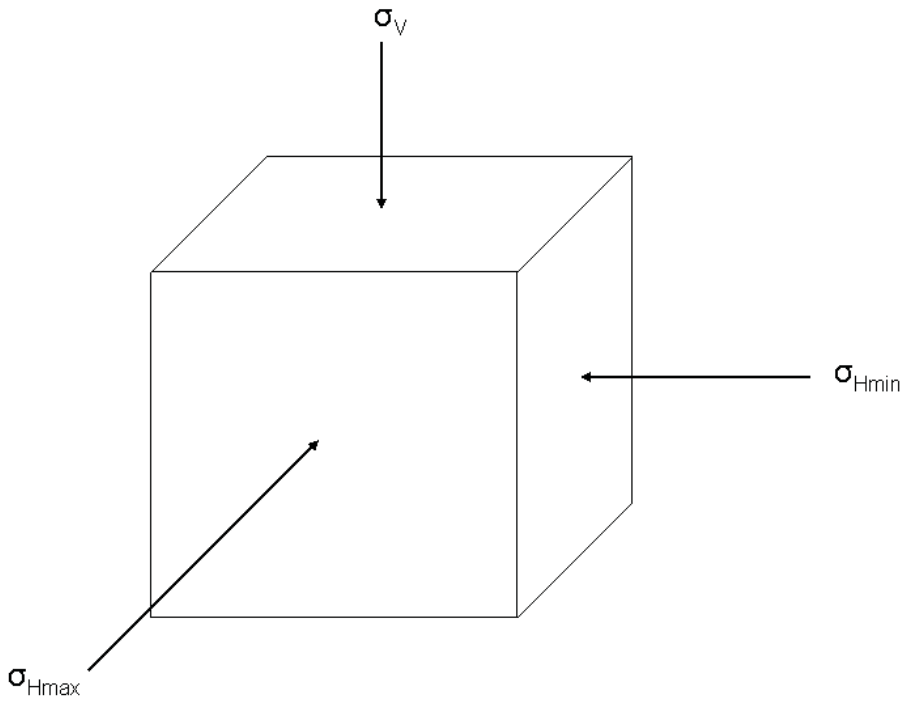

Figure 1: The three principal compressive stresses [8]

The vertical stress relates to the weight of overburden. At a given depth H, the vertical stress σ_v of the formation is defined by:

$$\sigma_v = g\int_0^H \rho_f \cdot dH \quad \text{.....(2)}$$

where ρ_f is the density of the overlaying formation. Taking the average density of the overburden formation, the *in-situ* stress in the vertical direction can be expressed as:

$$\sigma_v = \frac{\rho_f \cdot H}{144} \quad \text{.....(3)}$$

with σ_v in psi, ρ_f in lbm/ft³ and H in ft.

This expression is known as the absolute vertical stress in the porous medium. Since the overburden stress will be carried by both the grains and the fluid within the pore space, an effective stress must be defined as:

$$\sigma_v' = \sigma_v - \alpha \cdot p \quad \text{.....(4)}$$

where α is known as Biot's poro-elastic constant (approximately 0.7), and p is the pore pressure. To get the effective horizontal stress the vertical stress is translated horizontally by the use of Poisson's relationship:

$$\sigma_H' = \frac{\nu}{1-\nu}\sigma_v' \quad \text{.....(5)}$$

with Poisson's ratio ν (rock property, can be estimated from acoustic log data and lithology). The absolute horizontal stress would be:

$$\sigma_H = \sigma_H' + \alpha \cdot p \quad \text{.....(6)}$$

and decreases with fluid production. The magnitude of the effective horizontal stress may not be the same in all directions due to tectonic effects. Hence Eq. 6 is called the minimum horizontal stress and:

$$\sigma_{H\max} = \sigma_{H\min} + \sigma_{tect} \quad \text{.....(7)}$$

the maximum horizontal stress, where σ_{tect} is the tectonic stress [5, 7, 8].

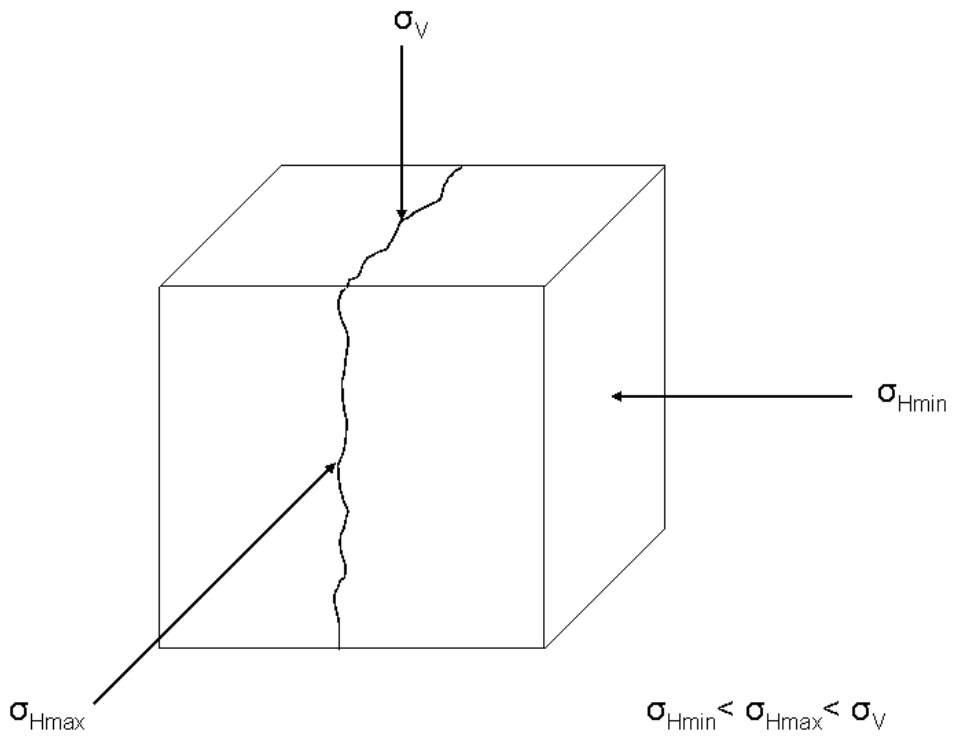

Figure 2: Fracture propagation [10]

The direction of a fracture will be perpendicular to the smallest of the three stresses, related to the minimum resistance. Depending on whether the least principal stress is horizontal, vertical or inclined, the hydraulic fracture will extend as vertical, horizontal or inclined, following the path of least resistance. Figure 2 suggests that the minimum horizontal stress σ_{Hmin} is smaller than the maximum horizontal stress σ_{Hmax} and smaller than the vertical stress σ_v. According to this stress relationship all hydraulic fractures should be vertical. In contrast, in shallow formations the least principal stress is the overburden stress. There the fractures should be horizontal [5, 8]. In Fig. 3 the stress magnitude is plotted as a function of depth. Here the change of a horizontal fracture to a vertical fracture due to the increasing overburden stress can be seen.

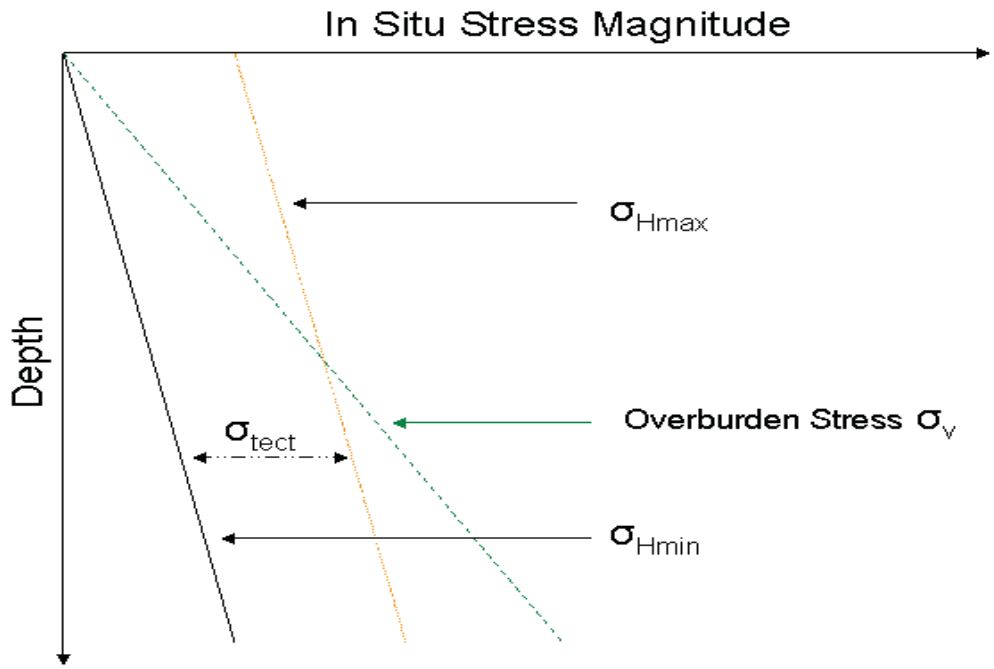

Figure 3: Stress magnitudes as a function of depth [5]

1.4 Fracture characterization

The most important factors in characterization of a hydraulic fracture are the skin effect, fracture conductivity and fracture length.

1.4.1 Skin effect

Invasion of drilling and completion fluids are some of the factors responsible for the reduction in permeability and creating a damaged zone in the vicinity of the well. This reduction can be expressed as an additional pressure drop Δp proportional to the production rate q:

$$\Delta p_{skin} = \frac{q\mu}{2\pi kh} s \quad \text{.....(8)}$$

The reduced permeability zone is known as the *skin*, the resulting effect on well performance is called *skin factor*. This invaded zone can reach between a few inches to several feet from the wellbore. The skin factor can be used as an indicator for the efficiency of well treatments. Its value can range between positive for damaged wells, caused by an additional pressure loss in the formation, negative for stimulated wells, and zero for a virgin, undamaged well. Theoretically, the skin factor of hydraulically fractured wells can vary from zero to a value as low as -7; practically skin factors up to -5.5 can be achieved by stimulation. Figure 4 illustrates the skin zone for a damaged well (s>0), an virgin, undamaged well (s=0), and a stimulated well (s<0).

The skin factor can be expressed by Hawkins formula:

$$s = \left(\frac{k}{k_s} - 1 \right) \ln \left(\frac{r_s}{r_w} \right) \quad \text{.....(9)}$$

where s is a function of the wellbore radius r_w, the radius of the damaged zone r_s, the reservoir permeability k and the permeability k_s of the skin zone [5, 6, 11]. Equation 8 indicates that a negative skin factor results in a negative Δp_{skin}. Hence, a stimulated well requires less pressure drawdown to produce at rate q than an equivalent well with uniform permeability. The value of the skin is dimensionless, and in most cases independent of flow rate, whereas the corresponding pressure drop Δp_{skin} is rate dependent.

In general, the pressure drawdown in the vicinity of a well can be expressed by:

$$\Delta p_{actual} = \Delta p_{ideal} + \Delta p_{skin} \quad \text{.....(10)}$$

where Δp_{ideal} represents the pressure drawdown of an undamaged well.

Considering the skin factor, the total steady state inflow equation becomes:

$$p_e - p_{wf} = \frac{q\mu}{2\pi hk} \left(\ln \frac{r_e}{r_w} + s \right) \quad \text{.....(11)}$$

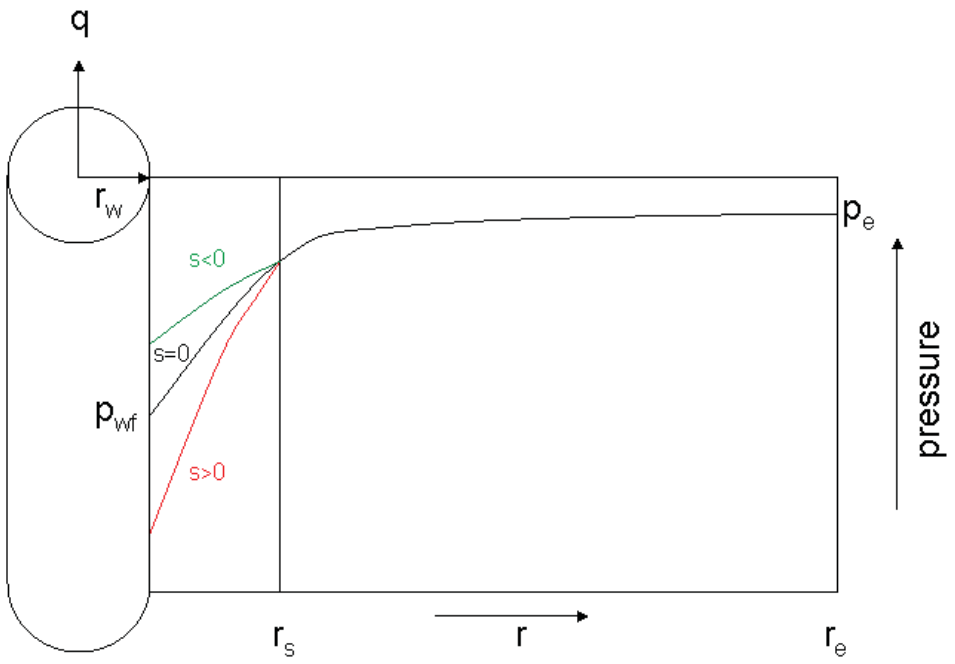

Figure 4: Radial pressure profile with skin effect [11]

1.4.2 Effective wellbore radius

The concept of the effective wellbore radius, r_{weff}, is to characterize the near-wellbore conditions in a more concrete way. It is a mathematical equivalent to the negative skin, and the relationship between the skin and the equivalent radius is:

$$r_{weff} = r_w \cdot e^{-s} \quad \text{.....(12)}$$

This term is used to describe the radius of an undamaged well with the same pressure drawdown like the damaged or stimulated well which is regarded. Thus, the productivity will be the same for the equivalent and the real well [5, 11, 12]. In Fig. 5 the effective wellbore radius is illustrated as a balancing of flow areas between the wellbore and the fracture [1].

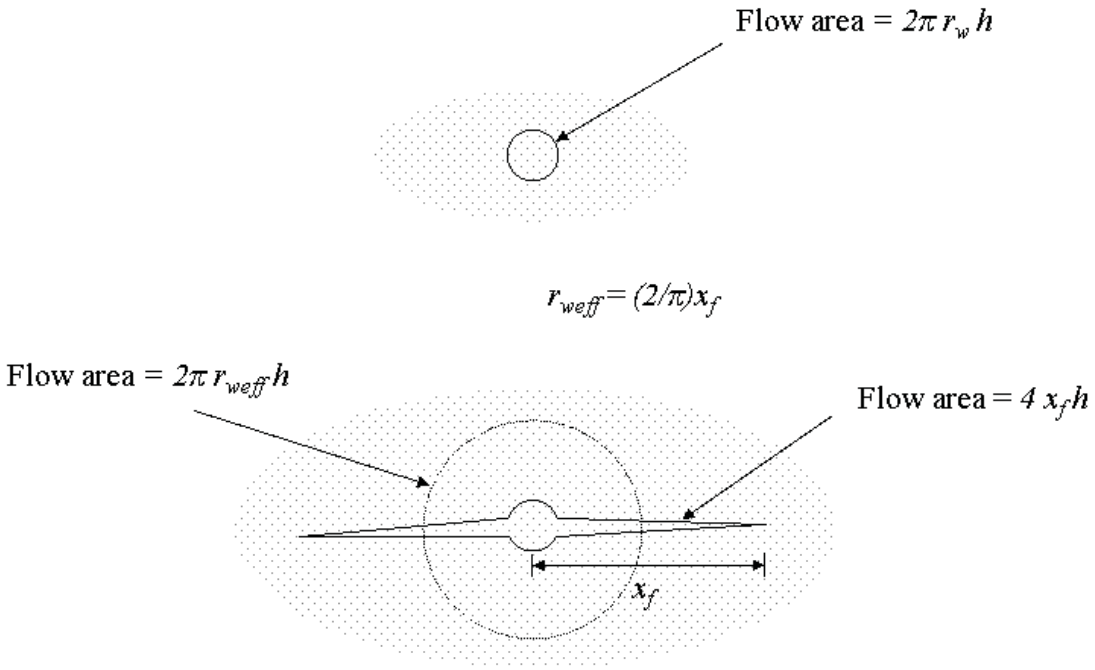

Figure 5: Concept of effective wellbore radius [1]

1.4.3 Conductivity

Another important term in fracture characterization is the fracture conductivity (Eq.13), which describes the ability of the fracture to transport the fluid divided by the ability of the formation to feed the fracture.

$$C_f = \frac{k_f \cdot w}{k \cdot x_f} \quad \text{.....(13)}$$

In the expression of the dimensionless conductivity C_f, k is the permeability of the reservoir, k_f the fracture permeability, w the width of the fracture and x_f the fracture half-length. Optimum fracture conductivity corresponds to the best compromise between fracture length and fracture width. The outcome of this is that low permeable formations

need a long and narrow fracture to result in optimal fracture conductivity, whereas high permeable formations require a short and wide fracture [5, 6].

1.5 Fracture models

The propagation and therefore the geometry of a fracture can be approximated by different models. These models combine elasticity, fluid flow, material balance and sometimes an additional propagation criterion considering mechanical properties of the rock, the properties of the fracturing fluid, the injection conditions (pressure, rate), and the stress field of the porous medium.

In general one can distinguish between three model families:

- 2D models
- Pseudo 3D models
- Fully 3D models

1.5.1 2D models

Planar 2D models are simplified by different assumptions. Their accuracies are limited due to the specified fracture height or the assumption of the fracture development. The simplest model is the radial or “penny-shaped” fracture model. This geometry occurs when the height growth is not limited by a barrier or when a horizontal fracture is created [5, 6].

1.5.1.1 The KGD model

In the Khristianovich and Zheltov (1955) and Geertsma and de Klerk (1969) model a fixed-height vertical fracture with an equal width along the wellbore is propagated in the vicinity of a well. All horizontal cross sections are identically and act independently or equivalently. Also the width of the fracture is assumed to change much slower along the vertical fracture face than horizontally. Thus the model is an acceptable approximation if the fracture length is much less than the fracture height ($x_f << h_f$). Furthermore the tip

region plays an important role, and the fluid pressure gradients in the fracture can be approximated [1, 5, 7]. The geometry of the KGD fracture model is illustrated in Fig. 6.

The average width of the KGD fracture is expressed as:

$$\overline{w} = 0.29\left[\frac{q_i \mu(1-\nu) x_f{}^2}{G h_f}\right]^{1/4}\left(\frac{\pi}{4}\right) \quad \text{.....(14)}$$

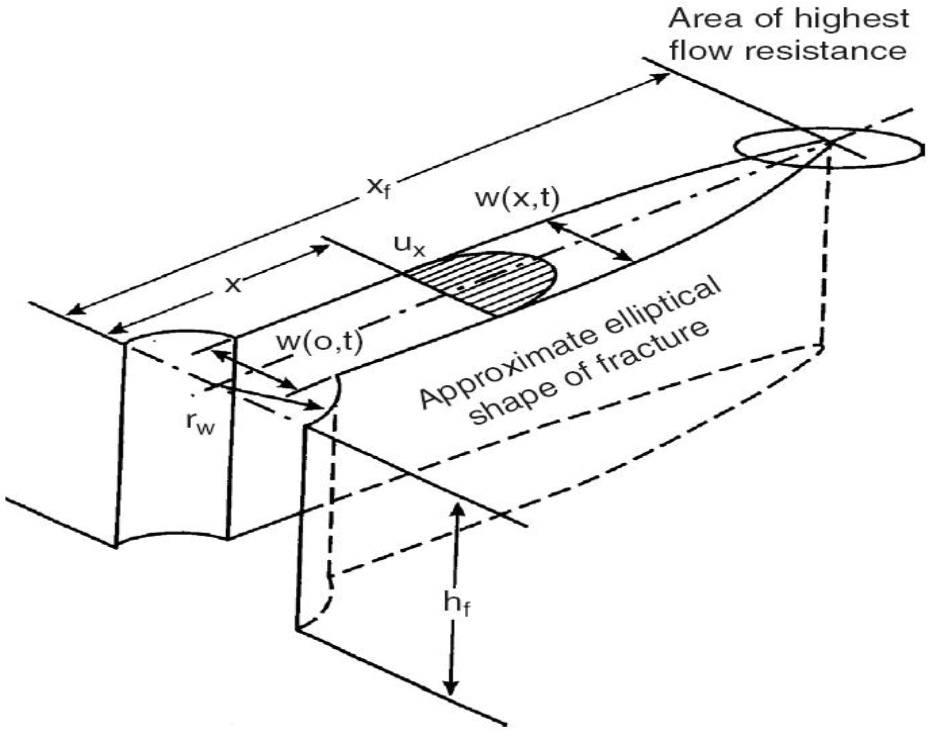

Figure 6: The KGD fracture geometry [7]

1.5.1.2 The PKN model

This model is a combination of the Perkins and Kern (1961) solution for a fixed-height vertical fracture and Nordgren's (1972) addition of leak off and storage within the fracture. The shape of the model at the wellbore is elliptical with the maximum width at the centerline of this ellipse and zero width at the top and the bottom. Each vertical cross section acts independently. Thus the model is true if the fracture length is much greater than the fracture height ($x_f >> h_f$). Unlike the KGD model, the fracture mechanics and tip

region are not considered [1, 5, 7]. Figure 7 demonstrates the geometry of the PKN fracture model.

Here the average width is expressed as:

$$\overline{w} = 0.3\left[\frac{q_i \mu(1-\nu)x_f}{G}\right]^{1/4}\left(\frac{\pi}{4}\gamma\right) \quad \text{.....(15)}$$

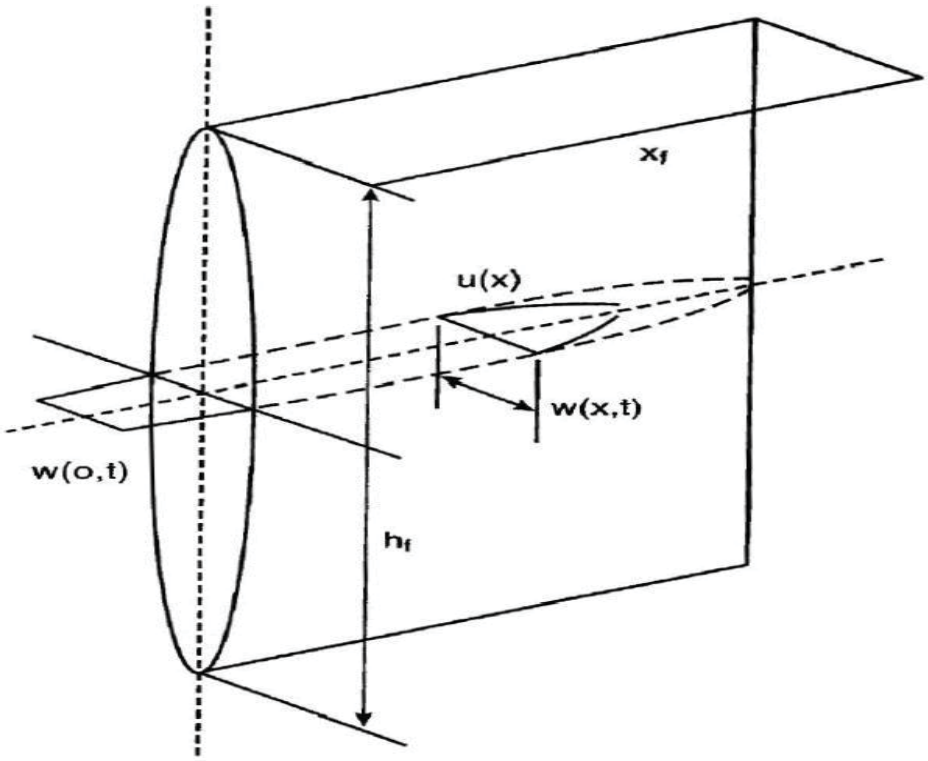

Figure 7: The PKN fracture geometry [7]

1.5.2 Pseudo 3D models

The problem of simple 2D models is that they require a specified fracture height, which is not always obvious from available data. Further, the fracture height varies in general from the well to the tip of the fracture. The pseudo-3D models are divided into two major types: lumped and cell based.

1.5.2.1 Lumped (elliptical) models

The vertical profile of the fracture consists of two half-ellipses which are connected at the center. For each time step the horizontal length and the vertical tip extensions of the wellbore are calculated. The basic assumption behind the model is that fluid flows along streamlines from the perforations to the edge of the ellipse. The shape of these streamlines is derived from simple analytical solutions and presented in Fig. 8 [1, 7].

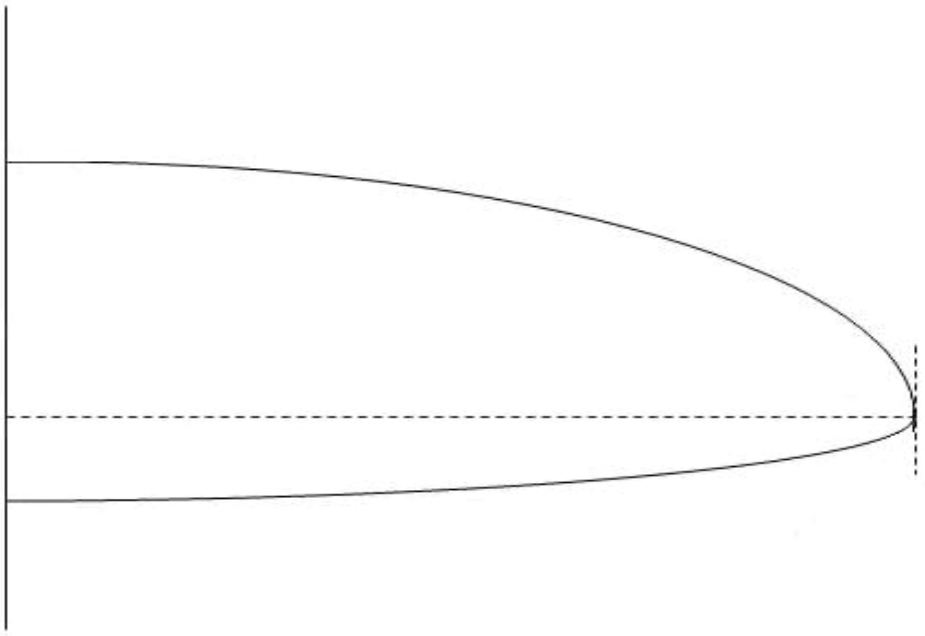

Figure 8: Vertical profile of a pseudo 3D lumped model [1]

1.5.2.2 Cell-based models

Discretization of the fracture length treats the fracture as a series of connected cells. Cell-based models do not prescribe the shape of the fracture but assume that each cell acts independently. The height growth of the fracture can be calculated, but the model is only a reasonable approximation if the length is much greater than the fracture height [1, 7].

1.5.3 Fully 3D models

In fully three dimensional models the fracture propagation can occur laterally and vertically with full two-dimensional fluid flow. Depending on different influencing factors like wellbore orientation, rock properties and perforation pattern the fracture direction may change the plane of the original direction in the beginning before orienting perpendicular to the minimum in-situ stress. Simulations based on such models require significant amounts of data and are extremely calculation intensive [1, 7].

The discussed fracture models are not very useful in a reservoir simulation model. As the fracture width and expansion is usually very small in contrast to the defined grid blocks, the implementation of the fractures is a scale problem.

1.6 Hydraulic fractures in a reservoir simulator

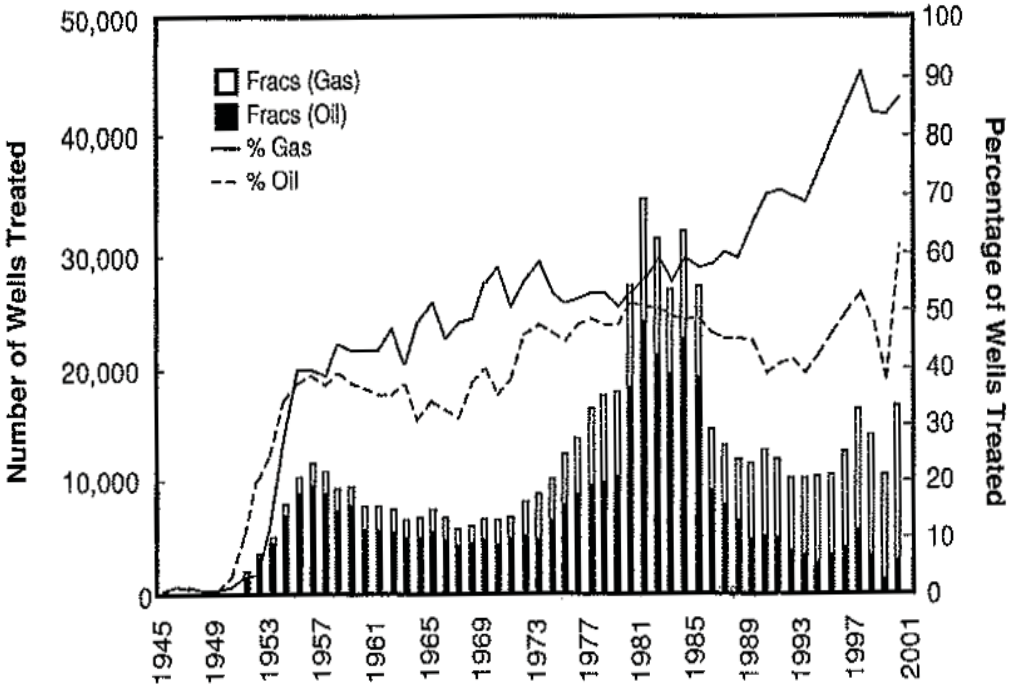

Figure 9: Fracturing as “completion of choice“ in U.S. oil and gas wells [13]

The interest in modeling hydraulic fractures has grown because the importance of well stimulation for the oil industry increased. Figure 9 illustrates the number of fractured gas

and oil wells in the U.S. from the year 1945 up to 2001. It shows that in 2001 nearly 90% of the drilled gas wells and more than 60% of the drilled oil wells are treated by a fracturing job.

The description of a hydraulic fractured well in a reservoir simulator turns out to be difficult. An accurate simulation of hydraulic fractures is only possible, if the reservoir discretization is very fine in the regions close to the fractures. Mostly, the fracture length is much smaller than the grid block containing the stimulated well, and the fracture properties are not considered explicitly in the simulation.

In general, hydraulically fractured wells are approximated by a negative skin or a modified productivity index. Also the effective wellbore radius can be increased in the simulation due to a stimulation treatment. However, none of these methods considers the fluid flow into and through the fracture. Furthermore the fracture direction is unnoticed; no difference can be made between a horizontal and a vertical fracture [14-17].

In the following examples the created fractures are incorporated in the simulation model by negative skin factors. The resulting consequences and problems are described in the subsequent chapter.

2 Problem definition

Under certain circumstances the simulation of a large negative skin factor in reservoir simulators (e.g. ECLIPSE) can lead to diverse problems. The simulation can run into convergence problems, can result in wrong outcome or even terminates abnormally. The cause of the simulation stop is that the effective radius of the well, r_{weff}, exceeds the pressure equivalent radius, r_0.

Due to these problems the basic idea is to find a mathematical relationship between the skin factor, the effective wellbore radius and the grid block geometry to estimate the maximum negative skin factor that can be run successfully in the simulation model.

After a short introduction about the basic simulation model two different ways for the estimation of the skin factor are discussed. The first possibility is based on an analytical experiment, the second on the Peaceman formula, introduced later in this chapter.

2.1 ODEH reservoir model

The ODEH data file from the Eclipse tutorials is used as a first example. This is the data for a three-dimensional gas/oil system, as described in [18], and represents a simple reservoir which is discretized into 10 x 10 x 3 grid blocks. All grid blocks have a side length of 1000 ft in the x- and y-direction. Only the thickness of the grid blocks varies from layer to layer (20, 30 and 50 ft) in the z-direction. Similarly, the permeability is constant within one layer, but varies with the different layers. Furthermore it consists of a gas injection well (r_w=0.25 ft) perforated in grid block (1, 1, 1) and a production well in grid block (10, 10, 3). The reservoir is located at a depth between 8325 and 8425 ft.

The simulation period takes 1200 days with fixed report times after 0, 1, 365, 730, 912.5, 1000, 1100 and 1200 days. Moreover the gas injection is kept at constant rate (100 000 Mscf/day).

Skin factor, permeabilities and geometry are altered during the experimental simulation runs. The complete data file is included in Appendix A. Figure 10 illustrates the geometry of the Odeh reservoir model.

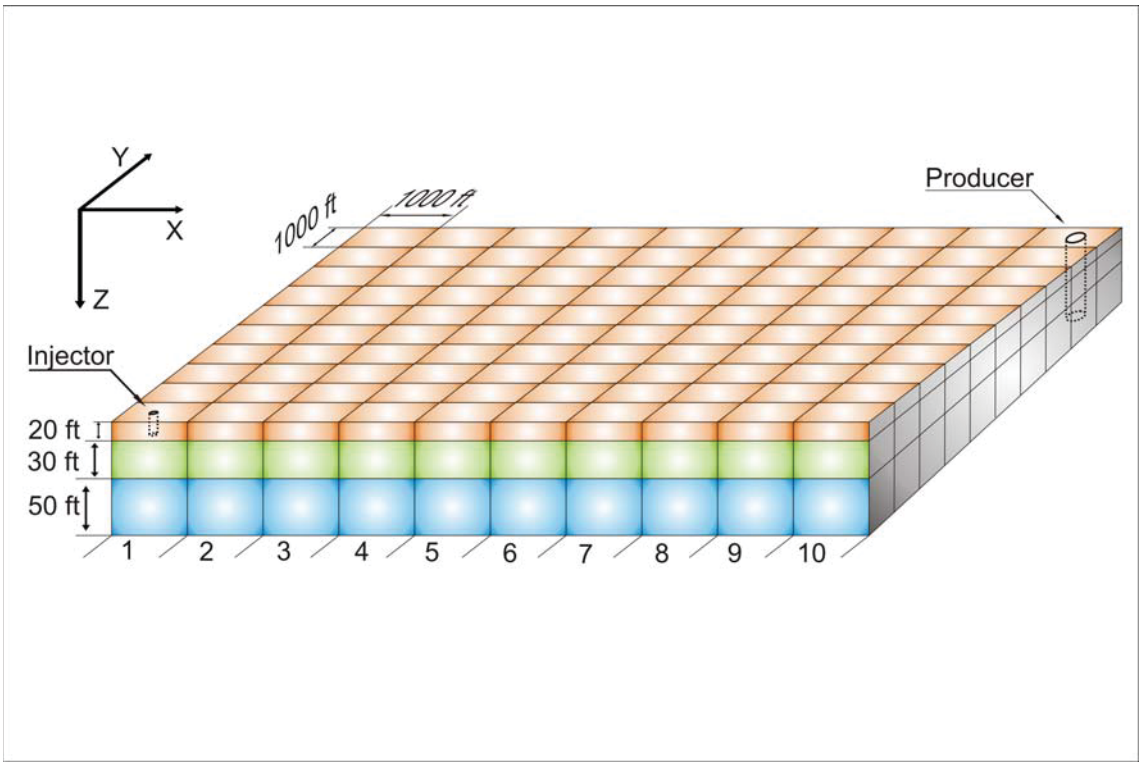

Figure 10: ODEH reservoir model

2.1.1 Skin variations

Based on the above discussed data file the influence of negative skin factors on the injector well bottomhole pressure is tested. Several simulation runs are done with decreasing skin factors between 0 and -7 with increments of 0.5. All other properties remain constant. From the results it appears that the skin factor of s = -6.6 is a threshold point for the simulation. Higher negative factors cause an abrupt simulation end. At a skin factor of s = -6.7 the following messages give information about the calculation stop:

```
@--  ERROR  AT TIME        0.0   DAYS    (19-OCT-1982):
 @           THE EFFECTIVE RADIUS OF WELL INJECTOR ( 203.10143)
 @           MUST BE LESS THAN THE PRESSURE EQUIVALENT RADIUS
 @           ( 197.98990) OF BLOCK    1   1   1. TOO MUCH NEGATIVE SKIN.


 @--  ERROR  AT TIME        0.0   DAYS    (19-OCT-1982):
```

```
@           UNREALISTIC CONNECTION DATA FOR CONNECTION    1   1   1
@           OF WELL INJECTOR.  EITHER THE WELL RADIUS
@           IS TOO BIG, OR THERE IS TOO MUCH NEGATIVE
@           SKIN.  THE CONNECTION FACTOR WILL BE NEGATIVE.
```

Figure 11 shows the change in bottomhole pressure with different skin values over time. An error bar at a range of ± 5% indicates the deviation of the different skin factors from the base case (s = 0). As can be seen the decreasing skin factors result in a decreasing bottomhole pressure of the injector well. The most significant difference due to varying skin factors is the well bottomhole pressure at day 1.

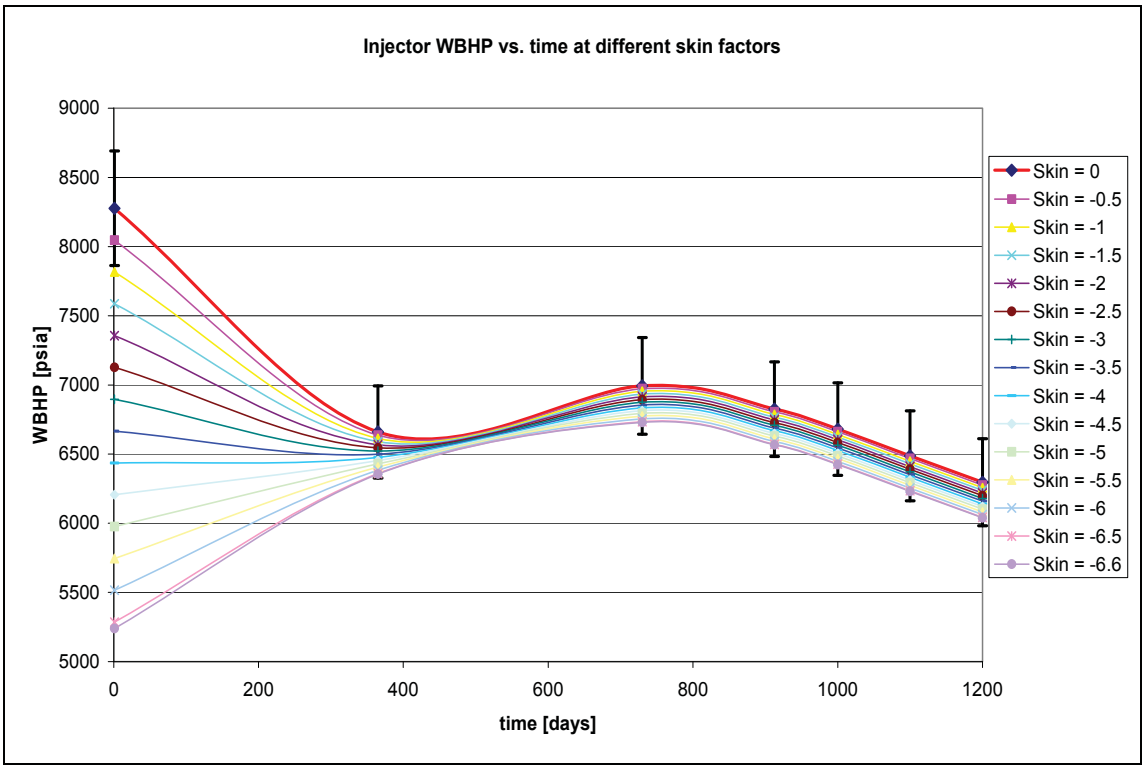

Figure 11: Influence of different skin factors on well bottomhole pressure

2.2 Analytical experiment

At first a relationship between the skin factor and the effective wellbore radius is detected. As mentioned in Eq. 12, the effective wellbore radius, r_{weff}, is only another mathematical notation of the skin factor and depends on the wellbore radius. For the analytical experiment the wellbore radius is kept constant (r_w= 0.25 ft) and the effective wellbore radius is calculated with skin values between 0 and -8 using Eq.12. Then the r_{weff} is plotted against the skin factor (Figure 12).

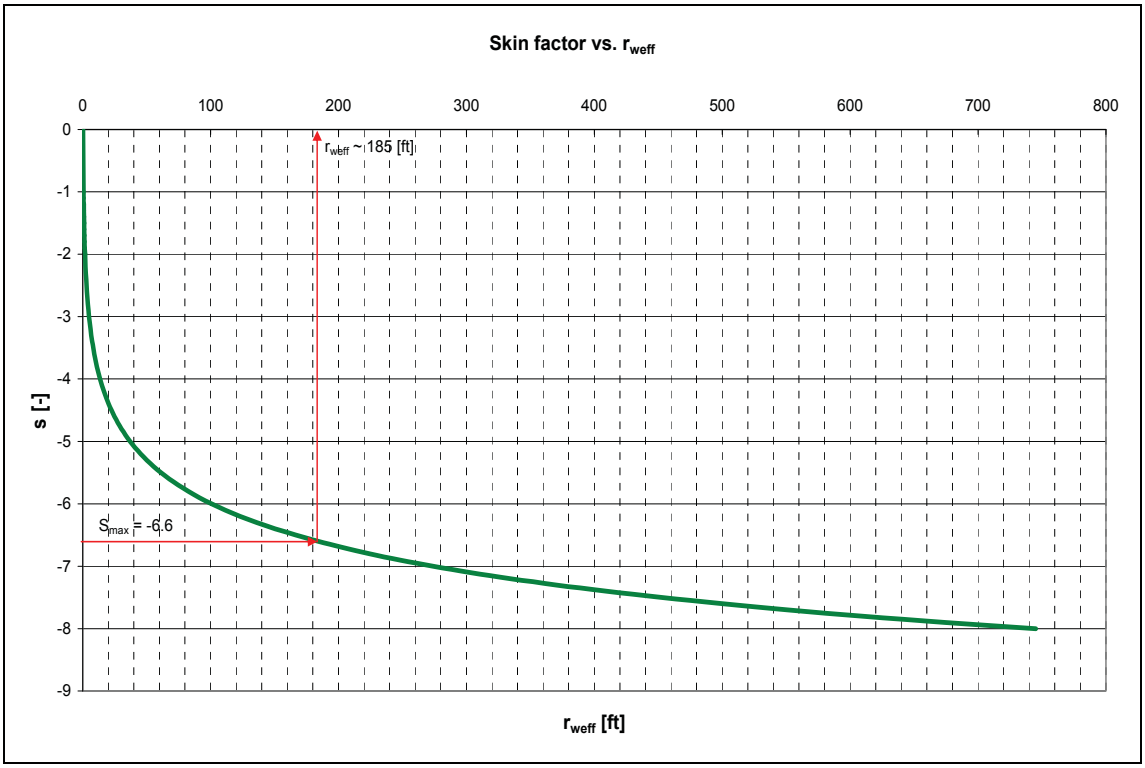

Figure 12: Skin factor vs. effective wellbore radius

Further the influence of the grid block geometry has to be determined. To get information about the grid block size limitation the data file is simulated with rising skin factors as long as the program brakes off. The thereby detected skin factor is used to determine the related effective wellbore radius by the calculated chart. For the next time the same procedure is done with changed Δx- and Δy-grid block values. Those changes are assumed to be randomly. After several runs with different grid block geometries a

relationship between the grid block diagonal d $\left(=\sqrt{\Delta x^2+\Delta y^2}\right)$ values and the skin related effective wellbore radius is detected by dividing this square root with the effective radius. All calculations result in a reasonable factor between 7.2 and 7.8 (Table 1). Assuming that this factor is a constant, the relationship between the constant and the effective wellbore radius is:

$$\frac{\sqrt{\Delta x^2+\Delta y^2}}{r_{weff}}=C \quad \text{.....(16)}$$

As the effective wellbore radius is defined by Eq. 12, the constant C becomes:

$$\frac{\sqrt{\Delta x^2+\Delta y^2}}{r_w\cdot e^{-s}}=C \text{.....(17)}$$

Consequently, the skin factor can be calculated from:

$$s=-\ln\left(\frac{\sqrt{\Delta x^2+\Delta y^2}}{C\cdot r_w}\right) \text{.....(18)}$$

The maximum value of C=7.80 results in a conservative estimation of the skin factor. Thus Eq. 18 can be rewritten as:

$$s\approx-\ln\left(\frac{\sqrt{\Delta x^2+\Delta y^2}}{7.8\cdot r_w}\right) \text{.....(19)}$$

Using this equation for estimation of the skin factor compares well with the maximum skin factor values from the simulation for different grid block sizes (Table 1).

The comparison between the simulated and the calculated highest negative skin factor for different grid block geometries can be seen in Fig. 13.

Δy [ft]	Δx [ft]	s_{max}*	r_{weff} [ft]	d [ft]	C_{calc}	s_{calc} with $C = 7.8$
10	50	-3.3	6.78	50.99	7.52	-3.26
20	50	-3.4	7.49	53.85	7.19	-3.32
33	50	-3.5	8.28	59.91	7.24	-3.42
100	75	-4.2	16.67	125.00	7.50	-4.16
90	90	-4.2	16.67	127.28	7.63	-4.18
60	120	-4.3	18.42	134.16	7.28	-4.23
100	130	-4.5	22.50	164.01	7.29	-4.43
100	144	-4.5	22.50	175.32	7.79	-4.50
125	500	-5.6	67.61	515.39	7.62	-5.58
270	500	-5.7	74.72	568.24	7.61	-5.67
290	500	-5.7	74.72	578.01	7.74	-5.69
300	500	-5.7	74.72	583.10	7.80	-5.70
350	500	-5.8	82.57	610.33	7.39	-5.75
400	500	-5.8	82.57	640.31	7.75	-5.79
450	500	-5.9	91.26	672.68	7.37	-5.84
100	1000	-6.3	136.14	1004.99	7.38	-6.24
549	887	-6.3	136.14	1043.15	7.66	-6.28
355	1234	-6.5	166.29	1284.05	7.72	-6.49
1432	1234	-6.9	248.07	1890.34	7.62	-6.88
1000	1000	-6.6	183.77	1414.21	7.70	-6.59

*s_{max} indicates the maximum negative skin factor that can be run successfully at a given geometry

Table 1: Relationship between skin, r_{weff} and grid block size (r_w = 0.25 [ft] for all cases)

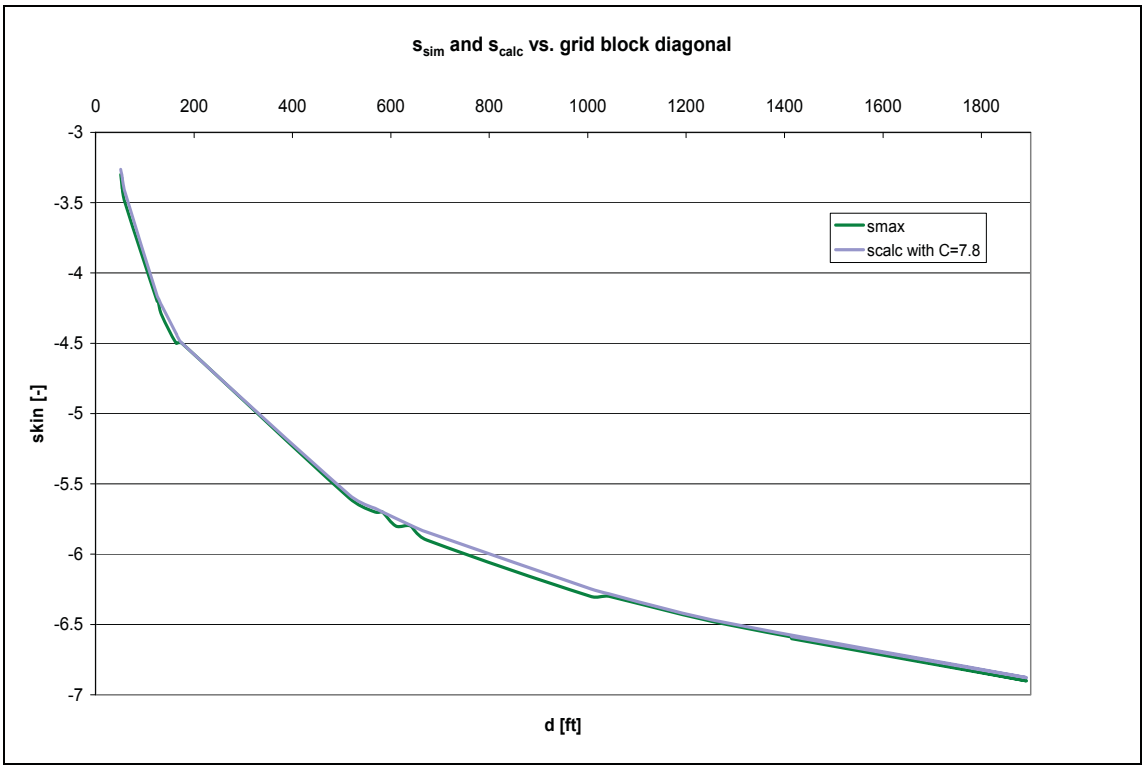

Figure 13: Maximum negative skin factor and calculated skin factor as a function of the grid block diagonal d

The result is a good estimation for the skin factor until the program breaks off. The use of the grid block diagonal allows the approximation for the skin also in rectangular and more complex geometries. Unfortunately, the estimated constant gives an inadequate solution if a really accurate answer about the skin factor is needed.

2.3 The pressure equivalent radius

The discretization of a reservoir leads to the problem that any grid block containing a vertical well has much larger lateral dimensions than the wellbore radius of that well. Therefore the calculated pressure for a grid block containing the well will be different from the well flowing bottomhole pressure. Peaceman (1978) introduced the idea of the pressure equivalent radius. The pressure equivalent radius (r_0) is defined as the distance from the well, at which the actual flowing pressure is equal to the numerically calculated

pressure of the block [19]. For steady-state and transient flowing conditions, the pressure equivalent radius, r_0, for a square grid is expressed by:

$$r_0 = 0.2 \cdot \Delta x \quad \text{.....(20)}$$

and more general for a non-square grid:

$$r_0 = 0.14 \cdot \left(\Delta x^2 + \Delta y^2\right)^{1/2} \quad \text{.....(21)}$$

where Δx and Δy are the grid dimensions [19].

For numerical reservoir simulations in an anisotropic medium, where either square or non-square grid blocks are used, the pressure equivalent radius is given by Eq. 22, known as Peaceman formula [20]:

$$r_0 = 0.28 \cdot \frac{\left[\left(\frac{k_y}{k_x}\right)^{1/2} \Delta x^2 + \left(\frac{k_x}{k_y}\right)^{1/2} \Delta y^2\right]^{1/2}}{\left(\frac{k_y}{k_x}\right)^{1/4} + \left(\frac{k_x}{k_y}\right)^{1/4}} \quad \text{.....(22)}$$

2.3.1 Square sized grid blocks

The first trial is made with a grid block dimension of 1000 x 1000 ft. To simplify the problem the reservoir consists only of one single layer with constant permeability in the x- and y-direction. Adapted from Eq. 22 the pressure equivalent radius is calculated and compared to the effective pressure chart for a well with 0.25 ft radius (Fig. 12). As long as the effective wellbore radius is less than the equivalent wellbore radius, the simulation runs without an error. At the point the effective wellbore radius exceeds the equivalent wellbore radius the simulation stops. Therefore the knowledge about the equivalent wellbore radius is fundamental for the forecast of the highest negative skin factor the program is able to simulate.

2.3.1.1 *Example:*

Input: square sized grid block:

Δx=Δy=1000 ft

r_w =0.25 ft

Therefore, the pressure equivalent radius is:

$$r_0 = 0.2 \cdot 1000\, ft = 200\, ft$$

According to Table 2 the largest skin factor that results in an effective wellbore radius smaller than 200 ft is -6.6. Higher negative skin values will tend to stop the simulation run. This result can be easily confirmed by simulation.

r_w [ft]	s	r_{weff} [ft]
0.25	0	0.25
0.25	-1	0.68
0.25	-1.5	1.12
0.25	-2	1.85
0.25	-2.5	3.05
0.25	-3	5.02
0.25	-3.5	8.28
0.25	-4	13.65
0.25	-4.5	22.50
0.25	-5	37.10
0.25	-5.5	61.17
0.25	-6	100.86
0.25	-6.2	123.19
0.25	-6.3	136.14
0.25	-6.5	166.29
0.25	-6.6	183.77
0.25	-6.7	203.10

Table 2: Skin vs. r_{weff} for r_w = 0.25 [ft]

2.3.2 Non-square sized grid blocks

In contrast to other pressure equivalent formulas, the Peaceman formula can also be utilized to describe r_0 in non-square geometries. Moreover, this formula also implies different permeabilities in x- and y-directions (anisotropic formation). Several runs are made with varying permeabilities and Δx- and Δy-values. Naturally, the permeability influences the calculation only if the k_x- and k_y-values are different. With the Peaceman formula the skin factor forecast is very accurate as long as Peaceman's well model is used in the simulator.

2.3.2.1 Example:

Input: r_w =0.25 ft

Δx = 500 ft

Δy = 730 ft

k_x = 500 mD

k_y = 350 mD

$$r_0 = 0.28 \cdot \frac{\left[\left(\frac{350}{500}\right)^{1/2} 500^2 + \left(\frac{500}{350}\right)^{1/2} 730^2\right]^{1/2}}{\left(\frac{350}{500}\right)^{1/4} + \left(\frac{500}{350}\right)^{1/4}} = 128.267\,ft$$

Comparing the calculated pressure equivalent radius to Table 2, the highest negative skin factor to simulate is -6.2.

In the next example, the concept is tested for a well with a wellbore radius of 0.5 ft.

2.3.2.2 Example:

Input: r_w = 0.5 ft

Δx = 500 ft

Δy = 730 ft

k_x = 500 mD

k_y = 350 mD

$$r_0 = 0.28 \cdot \frac{\left[\left(\frac{350}{500}\right)^{1/2} 500^2 + \left(\frac{500}{350}\right)^{1/2} 730^2\right]^{1/2}}{\left(\frac{350}{500}\right)^{1/4} + \left(\frac{500}{350}\right)^{1/4}} = 128.267\,ft$$

For a well with r_w=0.5 ft the maximum negative skin factor that can be simulated successfully is -5.5 (Table 3).

r_w [ft]	s	r_{weff} [ft]
0.5	0	0.5
0.5	-0.5	0.82436064
0.5	-1	1.35914091
0.5	-1.5	2.24084454
0.5	-2	3.69452805
0.5	-2.5	6.09124698
0.5	-3	10.0427685
0.5	-3.5	16.557726
0.5	-4	27.299075
0.5	-4.5	45.0085657
0.5	-5	74.2065796
0.5	-5.5	122.345966
0.5	-5.6	135.213204
0.5	-5.7	149.4337
0.5	-5.8	165.14978
0.5	-5.9	182.518734
0.5	-6	201.714397

Table 3: Skin vs. r_{weff} for r_w = 0.5 [ft]

2.4 Conclusion

To give a fast estimation about the highest possible negative skin, that can be simulated, the analytically detected formula gives a good solution, especially in simple geometries with constant permeabilities. Also the use of the grid block diagonal allows the use in non-square sized geometries. As the permeability is not considered in the equation, the result for anisotropic reservoirs is inaccurate.

Peaceman's formula on the other side allows an estimation of the skin factor also in anisotropic formations with varying permeabilities. The comparison of the pressure equivalent radius, r_0, and the effective wellbore radius, r_{weff}, makes the derivation of the maximum negative skin factor very easy.

3 Proposed solution

The calculation of the pressure equivalent radius with the Peaceman formula gives the possibility to derive the highest negative skin factor which can be used in the simulation without abnormal termination. If the desired skin factor is larger than this limit, then the question is how the simulation can be improved to match the intended skin factor. Three different multipliers are tested during the experiment until an adequate problem solution is found.

The test set-up is always the same for the three different multipliers. For each multiplier two runs are executed. In the first run the multipliers are always calculated as the ratio between an unstimulated well with a skin factor of zero and a stimulated well with a skin factor of s = -6. Each multiplier is included in the simulation data file with a skin factor of zero. In either case the resulting injector well bottomhole pressure is compared to the injector well bottomhole pressure of a simulation run with the basic Odeh data file, including a skin factor of s = -6. To prove the conclusion of the multipliers, also the ratio between a damaged well with skin factor s = +5 and the well with a skin factor of s = -6 is calculated in the second run. Naturally, the resultant multiplier is included in the data file with a skin of s = +5, and the outcome is also compared to the Odeh file, including a skin factor of s = -6.

3.1 Productivity index multiplier

The basic idea is to find the ratio between the productivity index of the reservoir produced with a positive or zero skin and a high negative skin. By definition the productivity index (PI) is the relationship between the production rate and the pressure drawdown in the vicinity of a well.

$$PI = \frac{q}{p_e - p_{wf}} = \frac{7.08 \cdot 10^{-3} kh}{\mu B_o \left(\ln \frac{r_e}{r_w} + s \right)} \quad \text{.....(23)}$$

The ratio between the original productivity index of the damaged or unstimulated well and the productivity index of the stimulated one is:

$$\frac{PI(s=new)}{PI(s=old)} = \frac{7.08\cdot10^{-3}\,kh}{\mu B_o\left(\ln\frac{r_e}{r_w}+s_{new}\right)}\cdot\frac{\mu B_o\left(\ln\frac{r_e}{r_w}+s_{old}\right)}{7.08\cdot10^{-3}\,kh} = \frac{\left(\ln\frac{r_e}{r_w}+s_{old}\right)}{\left(\ln\frac{r_e}{r_w}+s_{new}\right)} \quad \text{....(24)}$$

The thereby calculated value is used as a multiplier. This multiplier (*WPIMULT*) is included in the simulation data file in the schedule section.

3.1.1 Run 1

In the first run the ratio between the productivity index of the virgin, unstimulated well and the stimulated well is 3.61546. Used as a multiplier, this value is included in the simulation data file with a skin factor of zero. Subsequently, the bottomhole pressure of the injector well with a skin factor of s = -6 is compared to the well with zero skin, including the multiplier.

Multiplier calculation:

$$\frac{PI(s=-6)}{PI(s=0)} = \frac{\left(\ln\frac{1000}{0.25}+0\right)}{\left(\ln\frac{1000}{0.25}+(-6)\right)} = 3.61546$$

Data input in the schedule section:

```
-- INJECTION WELL CONTROLS
--
--      WELL      INJ    OPEN/  CNTL     FLOW
--      NAME     TYPE    SHUT   MODE     RATE
WCONINJE
     'INJECTOR' 'GAS' 'OPEN' 'RATE'  100000  /
  /
```

```
WPIMULT
      'INJECTOR' 3.61546 /
/
TSTEP
 2*365 182.5  87.5 100.0 100.0
  /
END============================================================
```

3.1.2 Run 2

For the second run the multiplier for a damaged well with a skin factor of s = +5 versus a well with a skin factor of s = -6 is calculated. Unlike the first run here the multiplier is used in combination with the original skin factor of the damaged well, s = +5.

Multiplier calculation:

$$\frac{PI(s=-6)}{PI(s=+5)} = \frac{\left(\ln\frac{1000}{0.25}+(+5)\right)}{\left(\ln\frac{1000}{0.25}+(-6)\right)} = 5.79501$$

3.1.3 Result

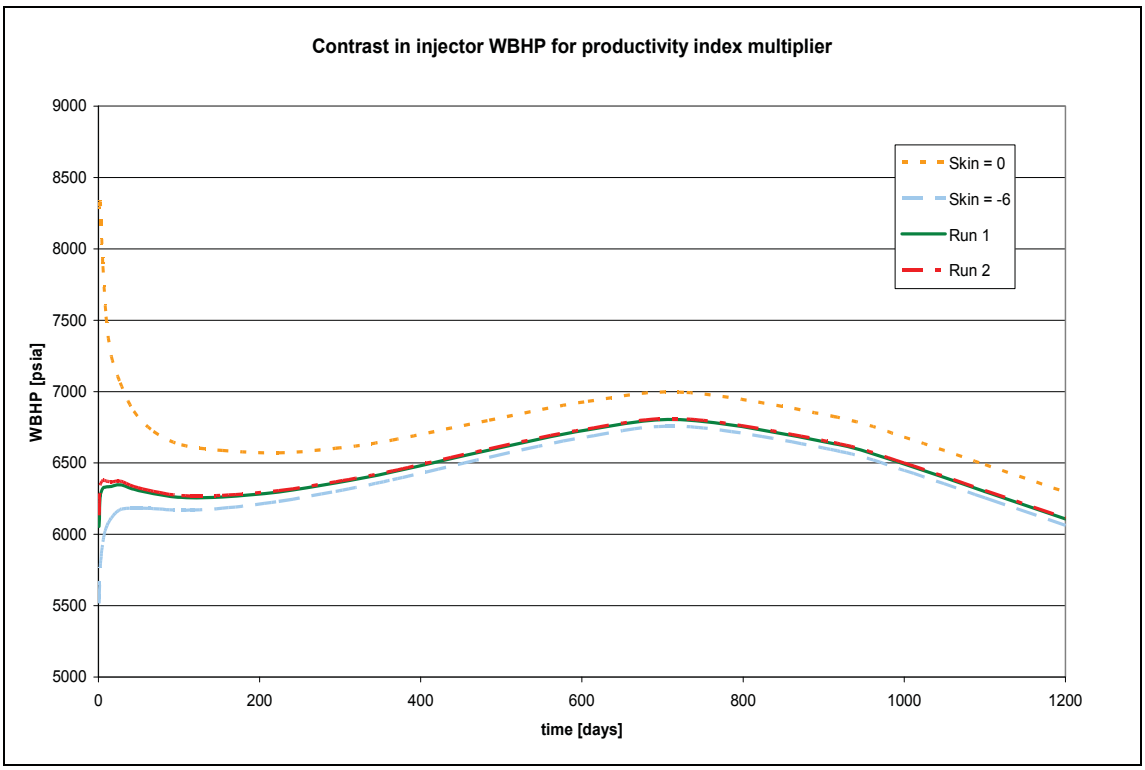

Figure 14: Contrast in injector WBHP for productivity index multiplier

Figure 14 illustrates the result of the two runs compared with the bottomhole pressure of the injector well for a skin factor of s = -6 and zero. At the beginning the productivity index multiplier 3.61546 (Run 1) is far away from the real well bottomhole pressure of the well with a skin factor of s = -6. The difference between both is always higher than 45 psi over the whole simulation time period and there is a great difference of more than 540 psi in the first 100 days of simulation. Nevertheless it is obvious, that the multiplier gives a rough approximation to the original behavior of the injector well bottomhole pressure.

The second run is hardly distinguishable from the first one. The output of a +5 skin factor compared with a multiplier (Run 2) offers also an inaccurate forecast how the injector well bottomhole pressure of a stimulated well with a skin factor of s = -6 behaves.

Besides the differences in the well bottomhole pressure, all other properties like field pressure, production rates or water cut remain identical, both in the stimulated and damaged or unstimulated case.

As the difference in injector well bottomhole pressure is significant, the productivity index multiplier is not a satisfactory method to avoid simulating a high negative skin factor.

3.2 Transmissibility multiplier

Another method of resolution is to increase the well block transmissibilities. The transmissibility between two adjacent grid blocks is simply a part of the flow coefficient. As a negative skin factor increases the flow rate due to an increased flow area, a higher transmissibility should have the same effect. Like in the productivity index multiplier, a ratio between the transmissibilities of a damaged or unstimulated well and a stimulated one is calculated and used as a multiplier.

ECLIPSE [2, 3] defines the transmissibility in the x-direction by:

$$TRANX_i = \frac{CDARCY \cdot TMLTX_i \cdot A \cdot DIPC}{B} \quad \text{.....(25)}$$

where

$TRANX_i$	is the transmissibility between cell (in positive x-direction)
$CDARCY$	is Darcy's constant (0.001127 in field units)
$TMLTX_i$	is a transmissibility multiplier for cell i
A	is the common interface area between cell i and cell j
$DIPC$	is the correction factor in the case of a dip
B	is the arithmetic average of DX/PERMX between cell i and cell j

Furthermore, the interface area, the dip correction and the factor B are expressed by:

$$A = \frac{DX_j \cdot DY_i \cdot DZ_i \cdot RNTG_i + DX_i \cdot DY_j \cdot DZ_j \cdot RNTG_j}{DX_i + DX_j} \quad \text{.....(26)}$$

$$B = \frac{\left(\frac{DX_i}{PERMX_i} + \frac{DX_j}{PERMX_j} \right)}{2} \quad \text{.....(27)}$$

$$DIPC = \frac{\left(\frac{DX_i + DX_j}{2} \right)^2}{\left(\frac{DX_i + DX_j}{2} \right)^2 + \left(DEPTH_i - DEPTH_j \right)} \quad \text{.....(28)}$$

From Darcy's equation for a phase p we know that:

$$q_p = CDARCY \cdot \frac{kA}{\Delta x} \frac{k_{rp}}{\mu_p} \Delta p \cdot \left(\ln\left(\frac{r_e}{r_w} \right) + s \right) \quad \text{.....(29)}$$

The term $\frac{k_{rp}}{\mu_p}$ is known as the relative mobility of a phase, λ_{rp}, and is a saturation-, pressure- and temperature- dependent term. $CDARCY \cdot \frac{kA}{\Delta x}$ is called the transmissibility *T*.

Consequently, q_p can also be written as:

$$q_p = T \cdot \lambda_{rp} \cdot \Delta p \left(\ln\left(\frac{r_e}{r_w} \right) + s \right) \quad \text{.....(30)}$$

To find a relationship between the transmissibility of the damaged or zero skin factor well and the well with a high negative skin, Eq. 30 must be rearranged to:

$$T = \frac{q_p \cdot \mu_p}{\Delta p \cdot k_{rp}} \left(\ln\left(\frac{r_e}{r_w} \right) + s \right) \quad \text{.....(31)}$$

Now, like in the productivity index multiplier the ratio between the original transmissibility of the damaged or unstimulated well and the transmissibility of the stimulated one is:

$$\frac{T(s=old)}{T(s=new)} = \frac{\frac{q_p \cdot \mu_p}{\Delta p \cdot k_{rp}}\left(\ln\left(\frac{r_e}{r_w}\right)+s_{old}\right)}{\frac{q_p \cdot \mu_p}{\Delta p \cdot k_{rp}}\left(\ln\left(\frac{r_e}{r_w}\right)+s_{new}\right)} = \frac{\left(\ln\left(\frac{r_e}{r_w}\right)+s_{old}\right)}{\left(\ln\left(\frac{r_e}{r_w}\right)+s_{new}\right)} \quad \text{.....(32)}$$

The result of Eq. 32 can be used as a transmissibility multiplier (*MULTX/MULTY*) in the simulation input file, included in the grid section, whereas the skin factor remains constant.

3.2.1 Run 3

The calculated multiplier (3.61546) is attached in the grid section to multiply both the permeabilities in x- and y-direction, while the skin factor remains zero. The bottomhole pressure of the injector well is compared to the results of a well with a skin factor of s = -6. Beside the bottomhole pressure also the field pressure is compared to the -6 skin factor well.

Multiplier calculation:

$$\frac{T(s=0)}{T(s=-6)} == \frac{\left(\ln\left(\frac{r_e}{r_w}\right)+0\right)}{\left(\ln\left(\frac{r_e}{r_w}\right)+(-6)\right)} = 3.61546$$

Data input in the grid section:

```
EQUALS
      'DX'    1000      /
      'DY'    1000      /
      'PORO'  0.3       /

      'DZ'    20        1  10  1  10  1  1  /
      'PERMX' 500       /
      'MULTX' 3.61546   /
```

```
'MULTY' 3.61546   /
'MULTZ' 0.64      /
'TOPS'  8325      /

'DZ'    30        1  10  1  10  2  2  /
'PERMX' 50        /
'MULTZ' 0.265625  /

'DZ'    50        1  10  1  10  3  3  /
'PERMX' 200       /
```

3.2.2 Run 4

As in run 2 the multiplier is calculated as the ratio between a well with a skin factor of s = -6 and a well with a skin factor of s = +5. For the input in the data file the multiplier is combined with a skin factor of s = +5.

Multiplier calculation:

$$\frac{T(s=+5)}{T(s=-6)} == \frac{\left(\ln\left(\frac{r_e}{r_w}\right)+(+5)\right)}{\left(\ln\left(\frac{r_e}{r_w}\right)+(-6)\right)} = 5.79502$$

3.2.3 Result

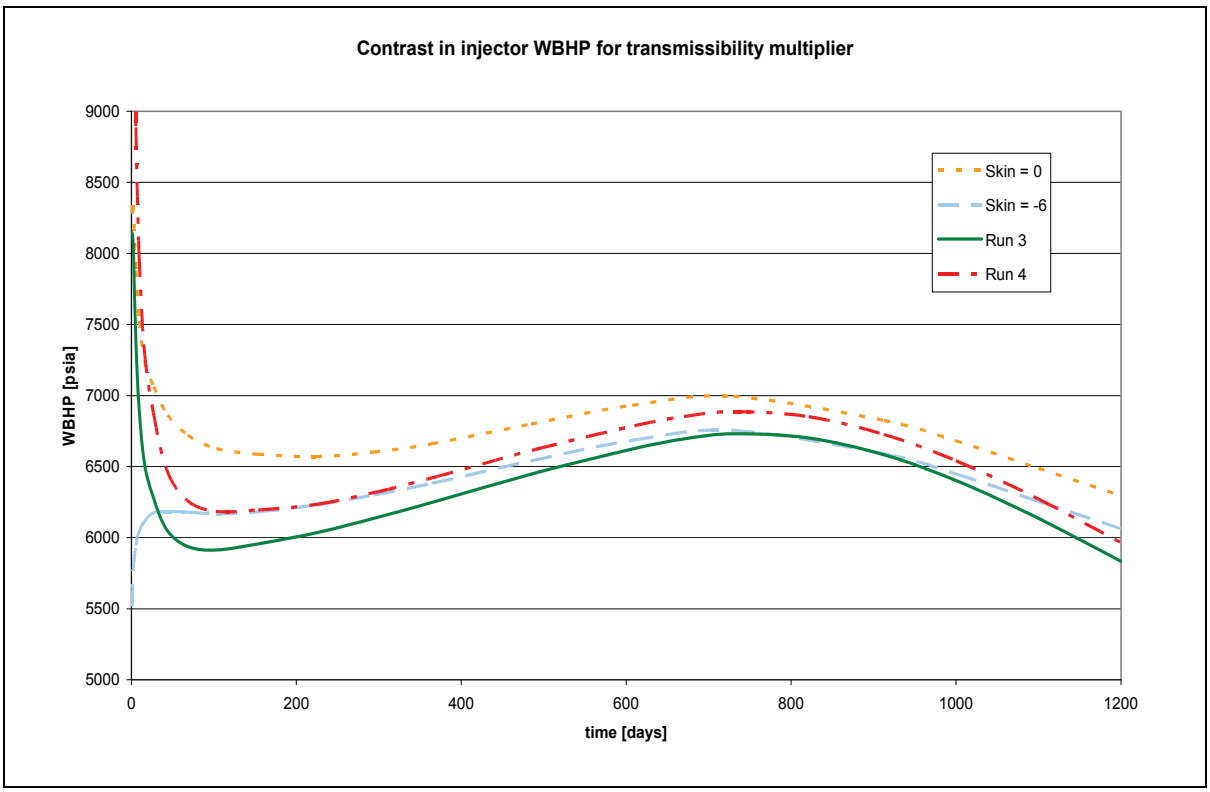

Figure 15: Contrast in injector WBHP for transmissibility multiplier

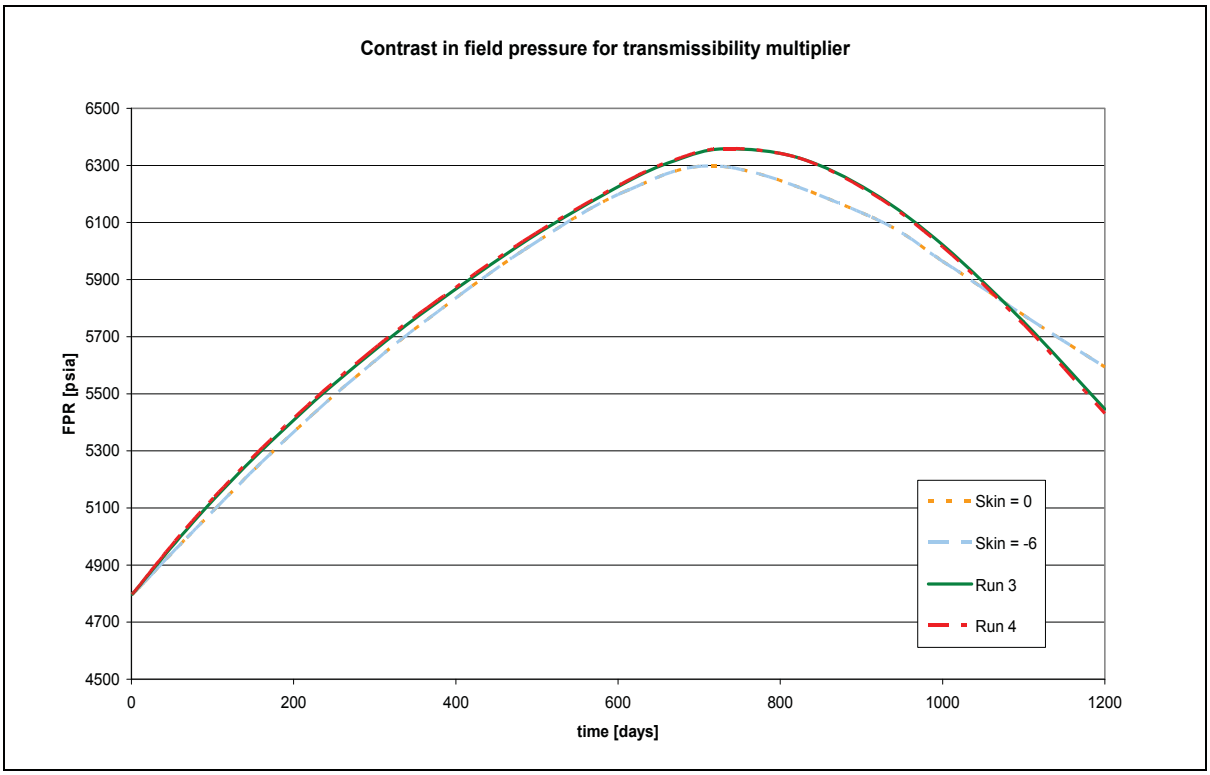

Figure 16: Contrast in field pressure for transmissibility multiplier

Figure 15 illustrates the contrast in injector well bottomhole pressure for different transmissibility multipliers and skin factors. Obviously, that the difference between the multiplier output and the output of a skin factor of s = -6 is significant. Most notably in the beginning is the difference between the well bottomhole pressure of the injector of multiplier 3.61546 (Run 3) and the well with skin factor s = -6 of more than 2600 psi, whereas the difference of multiplier 5.79502 (Run 4) is actually 5000 psi.

Also the shape of the two multiplier curves differs from the zero and -6 skin factor respectively. Comparing the zero curve to the -6 skin factor curve, the difference from 365 days on is more or less the same. By contrast varies the difference between the multiplier curves and the skin curves.

In Fig. 16 the contrast in field pressure is plotted. Normally, there should be no difference between the curves due to the comparatively short simulation time. However, there is a great difference in values and shape of the two multiplier curves and the skin factor curves right from the start. Therefore the transmissibility multiplier delivers no satisfactory solution to avoid a limiting skin factor.

3.3 Connection transmissibility factor

The transmissibility multiplier influences not only the pressure in the grid block containing the injection well, but also all properties of the other grid blocks. Therefore a multiplier influencing only the grid block containing the stimulated well is required. As the properties in the well grid block relate to the well inflow and outflow respectively, the relationship that the simulation program uses to calculate the well inflow performance is analyzed.

ECLIPSE [3] defines the flow path between the reservoir grid block containing the well and the well bore as a “connection”, and the Inflow Performance Relationship by:

$$q_{pj} = T_{wj} \cdot M_{pj} \cdot \left(P_j - P_w - H_{wj}\right) \quad \text{.....(33)}$$

where

q_{pj} is the volumetric flow rate of phase p (oil, water or gas) in connection j at stock tank conditions

T_{wj} is the connection transmissibility factor

M_{pj} is the phase mobility at the connection

P_j is the nodal pressure in the grid block containing the connection

P_w is the bottomhole pressure of the well

H_{wj} is the wellbore pressure head between the connection and the well's bottomhole datum depth

The most interesting factor is the connection transmissibility factor, T_{wj}, which is defined in Cartesian grids as:

$$T_{wj} = \frac{c\Theta kh}{\ln\left(\frac{r_0}{r_w}\right) + s} \quad \text{.....(34)}$$

and depends on the connecting grid block, the wellbore radius, and the rock permeability. The factor c is a unit conversion factor (0.001127 in field units). For the pressure equivalent radius calculation the Peaceman's formula (Eq. 22) is used [3].

To detect a multiplier for the connection transmissibility factor, the ratio between the old and the new connection factor is calculated by:

$$\frac{Twj(s = new)}{Twj(s = old))} = \frac{c\Theta kh}{\ln\left(\frac{r_0}{r_w}\right) + s_{new}} \cdot \frac{\ln\left(\frac{r_0}{r_w}\right) + s_{old}}{c\Theta kh} = \frac{\ln\left(\frac{r_0}{r_w}\right) + s_{old}}{\ln\left(\frac{r_0}{r_w}\right) + s_{new}} \quad \text{.....(35)}$$

This multiplier (*WPIMULT*) is included into the simulation file in the Schedule section.

3.3.1 Run 5

As the injector is penetrating only the first layer of the reservoir, the multiplier is calculated only with the permeability and height properties of this layer. The skin factor for the old well is assumed with zero, the compared skin factor for the stimulated well is -6. The results are illustrated in Fig. 17 and 18.

Multiplier calculation:

$$\frac{Twj(s=-6)}{Twj(s=0))} = \frac{\ln\left(\frac{197.99}{0.25}\right)+0}{\ln\left(\frac{197.99}{0.25}\right)+(-6)} = 9.89533$$

Data Input in the Schedule section:

```
-- INJECTION WELL CONTROLS
--
--      WELL      INJ    OPEN/   CNTL     FLOW
--      NAME     TYPE    SHUT    MODE     RATE
WCONINJE
     'INJECTOR' 'GAS' 'OPEN' 'RATE'  100000  /
  /
WPIMULT
      'INJECTOR' 9.89533 /

/
TSTEP
 2*365 182.5  87.5 100.0 100.0
  /

END     ============================================================
```

3.3.2 Run 6

To control the accuracy of the multiplier also for a damaged well, the multiplier is detected between a skin factor of s = +5 for the damaged well and a skin factor of s = -6 for the stimulated one. As input for the simulation a skin factor of s = +5 is used.

Multiplier calculation:

$$\frac{Twj(s=-6)}{Twj(s=+5)} = \frac{\ln\left(\frac{197.99}{0.25}\right)+5}{\ln\left(\frac{197.99}{0.25}\right)+(-6)} = 17.3081$$

3.3.3 Result

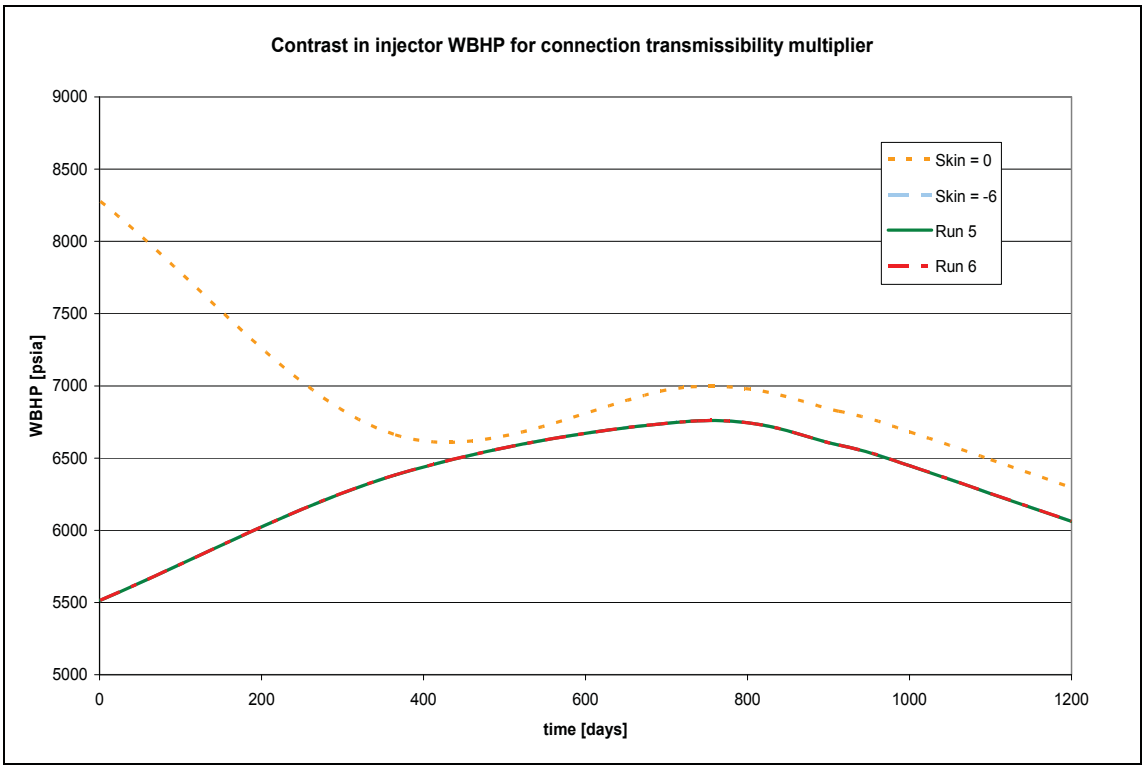

Figure 17: Contrast in injector WBHP for connection transmissibility multiplier

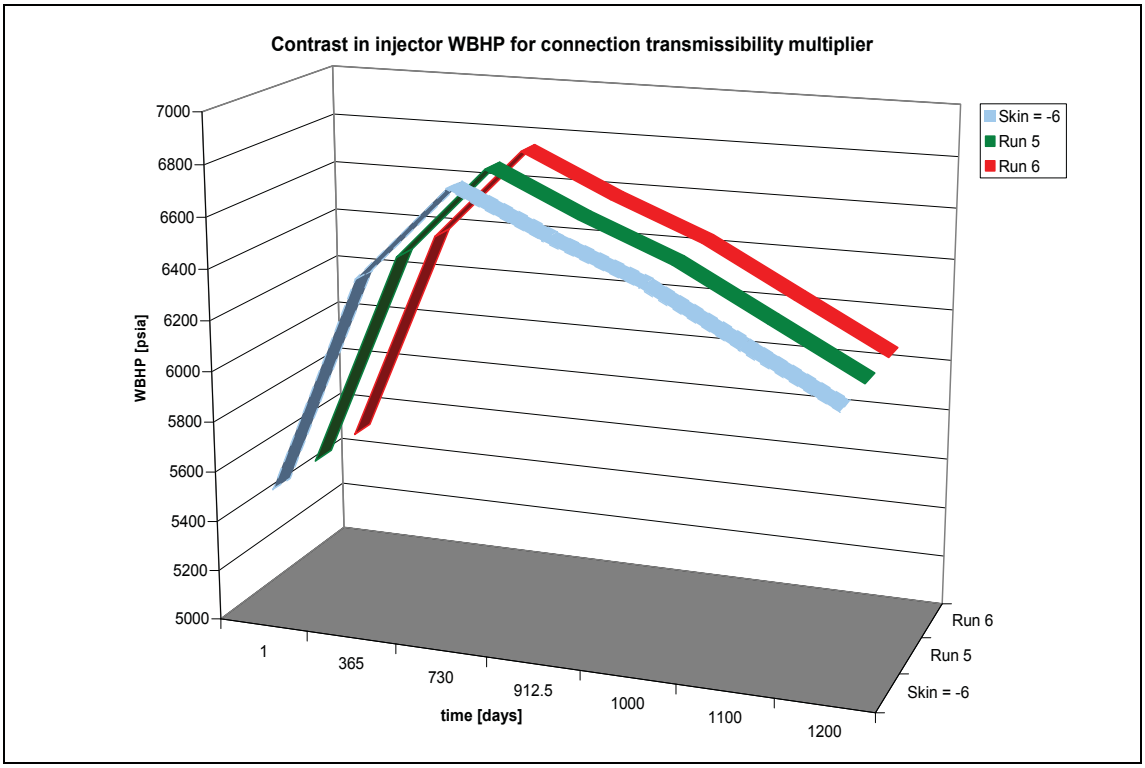

Figure 18: Contrast in injector WBHP for connection transmissibility multiplier in 3D

TIME [days]	Skin = -6 WBHP [psia] INJECTOR	Run 5 WPIMULT = 9.89533 WBHP [psia] INJECTOR	Run 6 WPIMULT = 17.3081 WBHP [psia] INJECTOR
0	4783.102	4783.102	4783.102
1	5515.432	5515.432	5515.432
365	6383.124	6383.124	6383.124
730	6754.28	6754.28	6754.28
912.5	6590.166	6590.166	6590.166
1000	6447.026	6447.027	6447.026
1100	6254.337	6254.337	6254.337
1200	6062.524	6062.524	6062.524

Table 4: Contrast in injector WBHP for connection transmissibility multiplier

Figure 17 and 18 picture the result of the connection transmissibility multiplier. Actually, the injector well bottomhole pressure over time coincides in all three simulation runs. In order to prove if the outcome is really the same, the well bottomhole pressure values of the injector well for the two multipliers and the skin factor of s = -6 are included in Table 4.

The connection transmissibility multiplier has no influence on properties of other grid blocks and is a very satisfactory tool to avoid a limiting high negative skin factor.

However, the calculation of the connection transmissibility factor requires an accurate knowledge of the well block geometry and permeability.

4 Application examples

Using the previously proposed way to successfully deal with high negative skin factors, some more runs are done with changing properties. The connection transmissibility factor seems to be applicable for easy geometries such as square sized grid blocks (Δx=Δy). Complex geometries on the other side present a more challenging situation.

4.1 Rectangular grid blocks

In the Odeh example the grid blocks are square sized. To proof the application of the connection transmissibility multiplier also for grid blocks with rectangular geometry, the data is altered to a 1000 x 1500 ft shape. The layer height remains the same.

4.1.1 Run 7

The new geometry is included in the grid section.

Input: r_w = 0.25 ft

Δx = 1000 ft

Δy = 1500 ft

k_x = 500 mD

k_y = 500 mD

Then the pressure equivalent radius, r_0, can be calculated from Eq.22:

$$r_0 = 0.28 \frac{\left[\left(\frac{500}{500}\right)^{1/2} 1000^2 + \left(\frac{500}{500}\right)^{1/2} 1500^2\right]^{1/2}}{\left(\frac{500}{500}\right)^{1/4} + \left(\frac{500}{500}\right)^{1/4}} = 252.389\,ft$$

Multiplier calculation for a skin factor of s = -6 (Eq. 35):

$$\frac{Twj(s=-6)}{Twj(s=0)} = \frac{\ln\left(\frac{252.389}{0.25}\right)}{\ln\left(\frac{252.389}{0.25}\right)+(-6)} = 7.54118$$

4.1.2 Run 8

If a damaged well (s = +5) is stimulated by a hydraulic fracturing job and the treatment results in a skin factor of s = -6, then the connection transmissibility multiplier becomes:

$$\frac{Twj(s=-6)}{Twj(s=+5)} = \frac{\ln\left(\frac{252.389}{0.25}\right)+5}{\ln\left(\frac{252.389}{0.25}\right)+(-6)} = 12.9922$$

4.1.3 Result

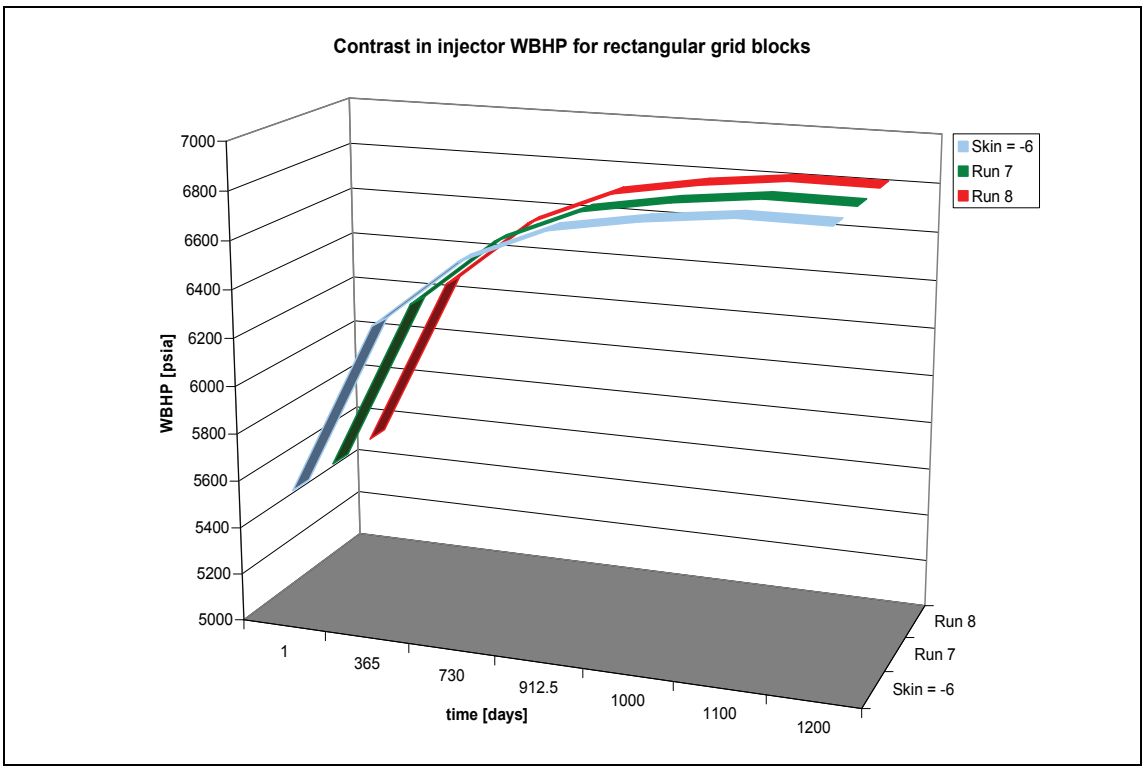

Figure 19: Contrast in injector WBHP for rectangular grid blocks

Figure 19 visualizes the comparison in well bottomhole pressure of three injector wells with different skin values and multipliers. Due to the rectangular shape of the grid blocks the equivalent wellbore radius is increased. This alteration influences the connection transmissibility multiplier. The output of an injector well with a skin factor of s = -6 is compared to an injector well with multiplier 7.54118 (Run 7) and a skin factor of zero, and an originally damaged well with multiplier 12.9922 (Run 8) and skin factor s = +5. In all three cases the output of the injector well bottomhole pressure is identical. Therefore, the connection transmissibility multiplier can also be used for rectangular grid block geometries.

4.2 Permeability anisotropy

In layers, where the permeabilities in x- and y-direction are equal, the permeability does not essentially influence the equivalent wellbore radius. Equation 22 reveals that the

permeability in z-direction, k_z, has no influence on the pressure equivalent radius, r_0, in vertical wells. The application of this equation in horizontal wells will be discussed later.

To prove the application of the connection transmissibility factor also for different k_x and k_y values, the following simulation run is arranged.

4.2.1 Run 9

The altered permeabilities are included in the grid section of the simulation data file.

Input: r_w = 0.25 ft

Δx = 1000 ft

Δy = 1000 ft

k_x = 500 mD

k_y = 300 mD

Pressure equivalent radius calculation (Eq.22):

$$r_0 = 0.28 \frac{\left[\left(\frac{300}{500}\right)^{1/2} 1000^2 + \left(\frac{500}{300}\right)^{1/2} 1000^2\right]^{1/2}}{\left(\frac{300}{500}\right)^{1/4} + \left(\frac{500}{300}\right)^{1/4}} = 199.581 ft$$

Multiplier calculation (Eq.35):

$$\frac{Twj(s=-6)}{Twj(s=0)} = \frac{\ln\left(\frac{199.581}{0.25}\right)}{\ln\left(\frac{199.581}{0.25}\right) + (-6)} = 9.79102$$

4.2.2 Run 10

The connection transmissibility multiplier for the altered permeability is calculated between a damaged well with skin factor s = +5 and a stimulated well with skin factor s = -6.

Multiplier calculation:

$$\frac{Twj(s=-6)}{Twj(s=+5)} = \frac{\ln\left(\frac{199.581}{0.25}\right)+5}{\ln\left(\frac{199.581}{0.25}\right)+(-6)} = 17.1169$$

4.2.3 Result

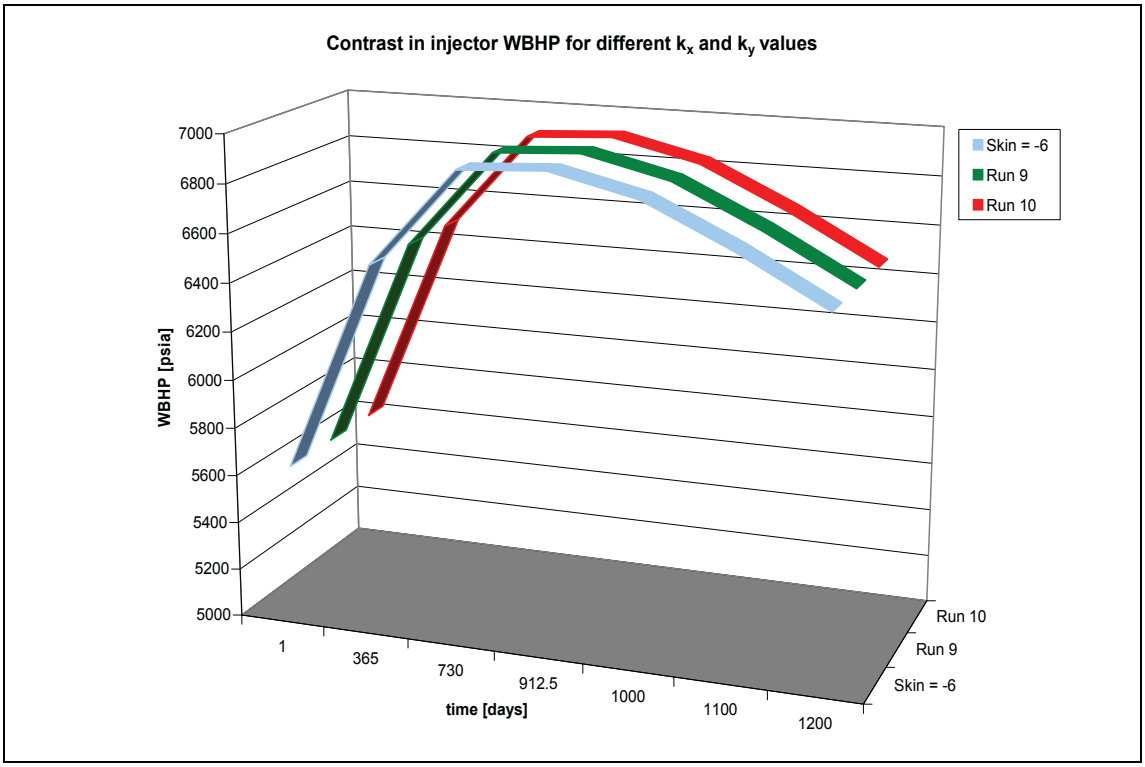

Figure 20: Contrast in injector WBHP for k_x = 500 mD and k_y = 300 mD

The alteration of the permeability influences the equivalent wellbore radius and therefore the value of the connection transmissibility multiplier. In Fig. 20 the contrast between the injector well bottomhole pressures of an unstimulated well with multiplier 9.79102, a damaged well with multiplier 17.1169 and a stimulated well with skin factor -6 is illustrated. Clearly, there is no difference in well bottomhole pressure between the three simulated

wells. Hence, the connection transmissibility multiplier is also useful in formations with different permeabilities in x- and y-direction.

4.3 Injector penetrating 3 layers

In the basic data file the injector well is penetrating only the first layer. To prove the application of the connection transmissibility multiplier also for wells perforated in several layers and therefore several grid blocks, the data is altered for an injector well penetrating all three layers of the reservoir. Furthermore, the permeabilities in the x- and y-direction are different in all three layers. As all layers have different permeabilities and heights, three different multipliers are calculated.

For the simulation some alterations are done in the Odeh data file.

First, the number of maximal connecting blocks needs to be increased, as the well is now penetrating three blocks in three layers.

```
WELLDIMS
    2    3    1    2 /
```

Then, the y-permeabilities are changed in all three layers.

```
EQUALS
      'DX'    1000      /
      'DY'    1000      /
      'PORO'  0.3       /

      'DZ'    20        1  10  1  10  1  1  /
      'PERMX' 500       /
      'PERMY' 300       /
      'MULTZ' 0.64      /
      'TOPS'  8325      /

      'DZ'    30        1  10  1  10  2  2  /
      'PERMX' 50        /
      'PERMY' 40       /
      'MULTZ' 0.265625  /

      'DZ'    50        1  10  1  10  3  3  /
      'PERMX' 200       /
      'PERMY' 300       /
```

Next, the injector bottomhole pressure depth is set to the center of the third grid block, to get the same scenario as in the examples before.

```
-- WELL SPECIFICATION DATA
--
--     WELL   GROUP LOCATION  BHP   PI
--     NAME   NAME    I  J   DEPTH DEFN
WELSPECS
    'PRODUCER' 'G'   10 10    8400 'OIL'  /
    'INJECTOR' 'G'    1  1    8400 'GAS'  /
/
```

The depth location of the injector is altered in the completion data.

```
-- COMPLETION SPECIFICATION DATA
--
--     WELL     -LOCATION- OPEN/ SAT CONN  WELL KH SKIN D-Factor DIR Ro

--     NAME     I  J K1 K2 SHUT  TAB FACT  DIAM
COMPDAT
    'PRODUCER'  10 10 3  3 'OPEN' 0   -1   0.5  1* -0    1*   'Z'  1* /
    'INJECTOR'   1  1 1  3 'OPEN' 1   -1   0.5  1* -0    1*   'Z'  1* /
 /
```

4.3.1 Run 11

The connection transmissibility multipliers are calculated between an unstimulated well (s = 0) and a stimulated well with skin factor s = -6 for all three layers. Beside the multipliers also the location of the well perforations are included in the simulation data file.

Input: r_w = 0.25 ft

Δx = 1000 ft

Δy = 1000 ft

Layer 1:

k_x = 500 mD

k_y = 300 mD

Pressure equivalent radius calculation (Eq.22):

$$r_0 = 0.28\frac{\left[\left(\frac{300}{500}\right)^{1/2}1000^2+\left(\frac{500}{300}\right)^{1/2}1000^2\right]^{1/2}}{\left(\frac{300}{500}\right)^{1/4}+\left(\frac{500}{300}\right)^{1/4}} = 199.581\,ft$$

Multiplier calculation (Eq.35):

$$\frac{Twj(s=-6)}{Twj(s=0)} = \frac{\ln\left(\frac{199.581}{0.25}\right)}{\ln\left(\frac{199.581}{0.25}\right)+(-6)} = 9.79102$$

Layer 2:

k_x = 50 mD

k_y = 40 mD

Pressure equivalent radius calculation (Eq.22):

$$r_0 = 0.28\frac{\left[\left(\frac{40}{50}\right)^{1/2}1000^2+\left(\frac{50}{40}\right)^{1/2}1000^2\right]^{1/2}}{\left(\frac{300}{500}\right)^{1/4}+\left(\frac{500}{300}\right)^{1/4}} = 198.297\,ft$$

Multiplier calculation (Eq.35):

$$\frac{Twj(s=-6)}{Twj(s=0)} = \frac{\ln\left(\frac{198.297}{0.25}\right)}{\ln\left(\frac{198.297}{0.25}\right)+(-6)} = 9.87495$$

Layer 3:

k_x = 200 mD

k_y = 300 mD

Pressure equivalent radius calculation (Eq.22):

$$r_0 = 0.28 \frac{\left[\left(\frac{300}{200}\right)^{1/2} 1000^2 + \left(\frac{200}{300}\right)^{1/2} 1000^2\right]^{1/2}}{\left(\frac{300}{200}\right)^{1/4} + \left(\frac{200}{300}\right)^{1/4}} = 198.998\, ft$$

Multiplier calculation (Eq.35):

$$\frac{Twj(s=-6)}{Twj(s=0)} = \frac{\ln\left(\frac{198.998}{0.25}\right)}{\ln\left(\frac{198.998}{0.25}\right) + (-6)} = 9.82886$$

```
WCONINJE
     'INJECTOR' 'GAS' 'OPEN' 'RATE'  100000  /
  /
WPIMULT
      'INJECTOR' 9.79102 1* 1* 1/
      'INJECTOR' 9.87495 1* 1* 2/
      'INJECTOR' 9.82886 1* 1* 3/
/
TSTEP
 2*365 182.5  87.5 100.0 100.0
  /


END     ============================================================
```

4.3.2 Run 12

The three different multipliers are also calculated for comparison of a damaged well with a skin factor of s = +5 and a stimulated well with skin factor s = -6.

Layer 1: WPIMULT (s_{old} = +5 and s_{new} = -6) = 17.1169

Layer 2: WPIMULT (s_{old} = +5 and s_{new} = -6) = 17.2707

Layer 3: WPIMULT (s_{old} = +5 and s_{new} = -6) = 17.1863

4.3.3 Result

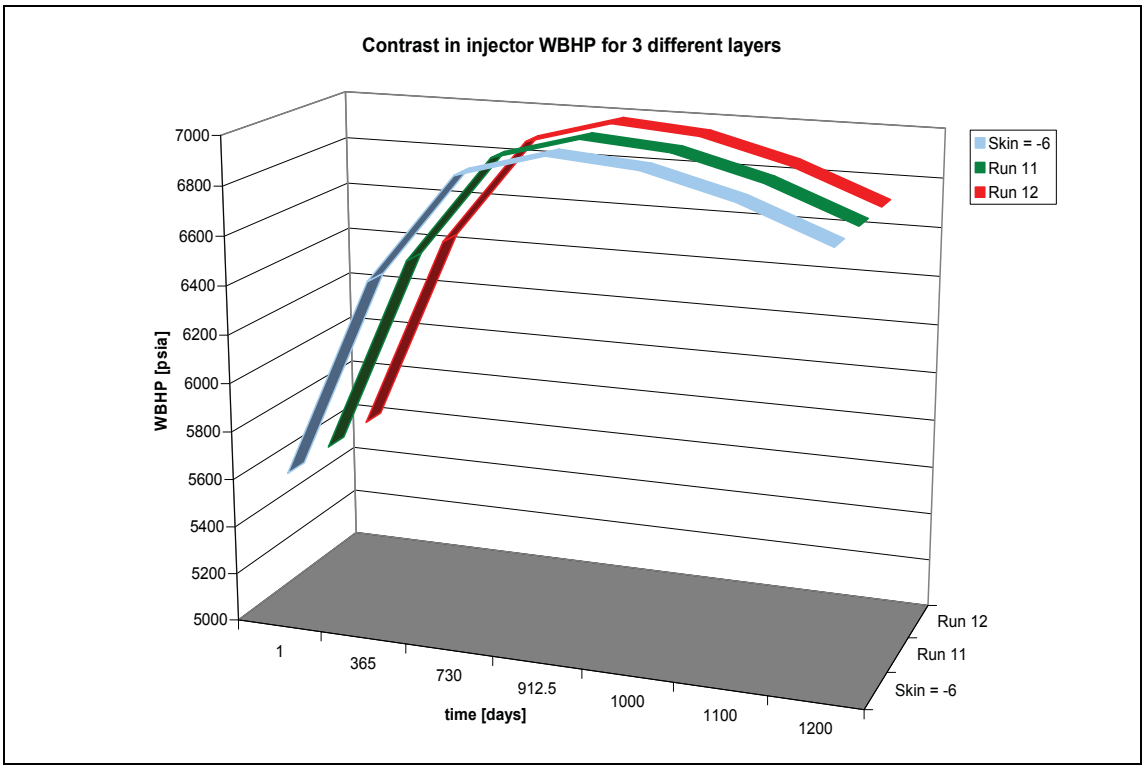

Figure 21: Contrast in injector WBHP for 3 different layers

The result of the simulation of a well penetrating three layers is illustrated in Fig. 21. Obviously, the two different multipliers for an undamaged and a damaged well deliver the same output as a stimulated well with a skin factor of s = -6.

The calculation of the connection transmissibility multiplier needs an accurate knowledge about the grid block geometry and properties of the involved blocks. In complex geometries, the implementation of the essential variables can easily be handled by a computer program.

4.4 Different skin factors

In the above example, the conclusion proves the fact that the connection transmissibility multiplier is also applicable if the well penetrates more than one grid block. As the skin factors are the same in all three penetrated grid blocks, the pressure equivalent radius, r_0, is almost the same for all three layers. To test the concept of the connection transmissibility multiplier under extreme conditions, the skin factors of the three penetrated layers are different in the next example.

4.4.1 Run 13

The model consists of three layers with three different skin factors. It is assumed that the skin factor of each layer can be improved by -3 due to a hydraulic fracturing job.

Input: r_w = 0.25 ft

Δx = 1000 ft

Δy = 1000 ft

Layer 1:

k_x = 500 mD

k_y = 300 mD

s_{old}= +3

s_{new}= 0

Pressure equivalent radius calculation (Eq.22):

$$r_0 = 0.28\frac{\left[\left(\frac{300}{500}\right)^{1/2}1000^2+\left(\frac{500}{300}\right)^{1/2}1000^2\right]^{1/2}}{\left(\frac{300}{500}\right)^{1/4}+\left(\frac{500}{300}\right)^{1/4}} = 199.581\,ft$$

Multiplier calculation (Eq.35):

$$\frac{Twj(s=+3)}{Twj(s=0)} = \frac{\ln\left(\frac{199.581}{0.25}\right)+3}{\ln\left(\frac{199.581}{0.25}\right)} = 1.44893$$

Layer 2:

k_x = 50 mD

k_y = 40 mD

s_{old}= -2

s_{new}= -5

Pressure equivalent radius calculation (Eq.22):

$$r_0 = 0.28\frac{\left[\left(\frac{40}{50}\right)^{1/2}1000^2+\left(\frac{50}{40}\right)^{1/2}1000^2\right]^{1/2}}{\left(\frac{300}{500}\right)^{1/4}+\left(\frac{500}{300}\right)^{1/4}} = 198.297\,ft$$

Multiplier calculation (Eq.35):

$$\frac{Twj(s=-5)}{Twj(s=-2)} = \frac{\ln\left(\frac{198.297}{0.25}\right)+(-2)}{\ln\left(\frac{198.297}{0.25}\right)+(-5)} = 2.78991$$

Layer 3:

k_x = 200 mD

k_y = 300 mD

s_{old}= -3

s_{new}= -6

Pressure equivalent radius calculation (Eq.22):

$$r_0 = 0.28 \frac{\left[\left(\frac{300}{200}\right)^{1/2} 1000^2 + \left(\frac{200}{300}\right)^{1/2} 1000^2\right]^{1/2}}{\left(\frac{300}{200}\right)^{1/4} + \left(\frac{200}{300}\right)^{1/4}} = 198.998\, ft$$

Multiplier calculation (Eq.35):

$$\frac{Twj(s=-6)}{Twj(s=-3)} = \frac{\ln\left(\frac{198.998}{0.25}\right) + (-3)}{\ln\left(\frac{198.998}{0.25}\right) + (-6)} = 5.41443$$

4.4.2 Result

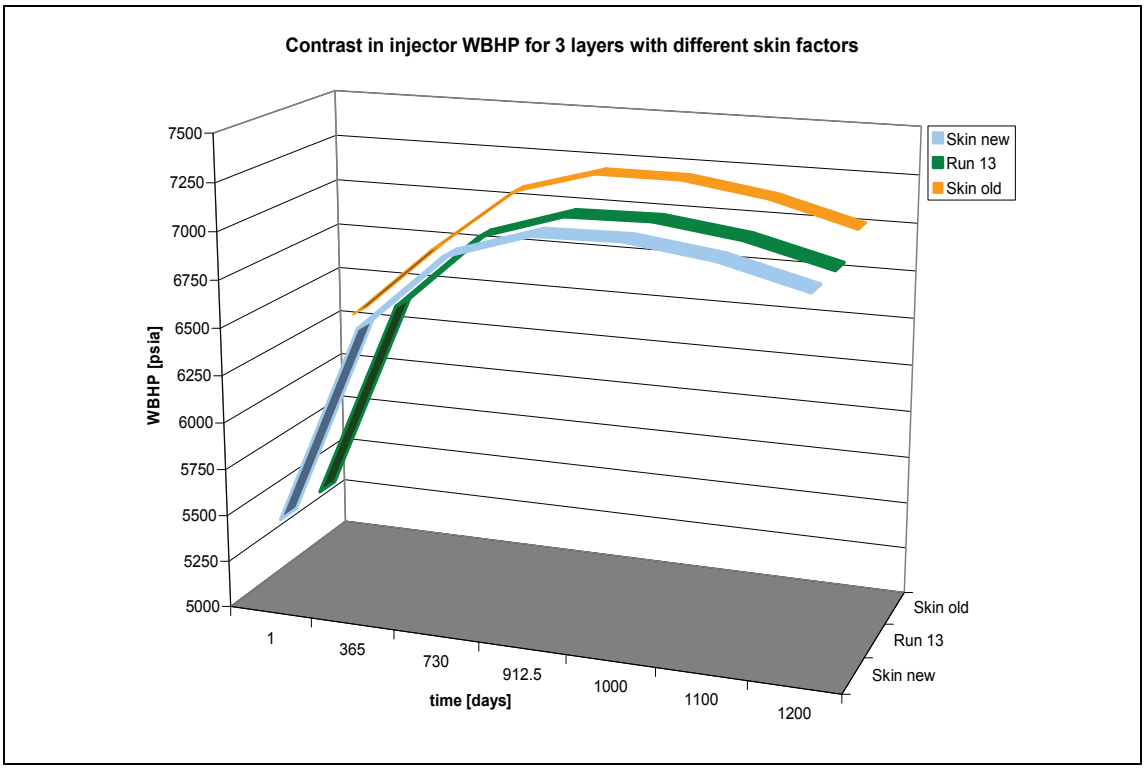

Figure 22: Contrast in injector WBHP for 3 layers with different skin factors

In Fig. 22 the bottomhole pressure of the injector well with new skin factors is compared to the multiplier run. The original well bottomhole pressure of the injector well is also illustrated. Even in this extreme test the connection transmissibility multiplier delivers the same result as the implementation of a new skin factor.

The conclusion proves the fact that the connection transmissibility multiplier is also applicable if the well penetrates more than one grid block with different grid block properties.

4.5 Horizontal well

The previous experiments show that the connection transmissibility multiplier is useful in vertical wells with different permeabilities and geometries. In the next runs the multiplier is tested for a horizontal well.

Primarily in tight gas and oil reservoirs and in coal beds, horizontal wells are good candidates. A larger and more efficient drainage pattern leads to an increased overall recovery, and productivity benefits of 10 times more compared to vertical wells could be achieved.

In hydraulic fracturing simulation, a horizontal well can be treated like a vertical well, if the complete wellbore with its hydraulic fractures is located within a single grid block. The concept of the effective wellbore radius is applicable, if the pressure equivalent radius of the grid block is higher than the effective wellbore radius (as explained in Chapter 3).

Peaceman's formula (Eq.22) assumes single phase flow, uniform grid block geometry and uniform permeability, homogenous formation and an isolated well (no influence of boundaries). The accuracy of the formula is very limited in horizontal wells, as in thin reservoirs a horizontal well can not be far from the top or bottom boundary, and the flow around the well may not be two-dimensional.

To diminish the influence of the boundary the data is altered to a well penetrating three grid blocks in the x-direction with the well shoe in grid block (2, 2, 1).

```
-- WELL SPECIFICATION DATA
--
--     WELL   GROUP LOCATION  BHP   PI
--     NAME   NAME    I  J   DEPTH DEFN
WELSPECS
    'PRODUCER' 'G'   10 10    8400 'OIL'  /
    'INJECTOR' 'G'    2  2    8335 'GAS'  /
/

-- COMPLETION SPECIFICATION DATA
--
--     WELL     -LOCATION- OPEN/ SAT CONN  WELL KH SKIN D-Factor DIR Ro

--     NAME     I  J K1 K2 SHUT  TAB FACT  DIAM
COMPDAT
    'PRODUCER'  10 10 3  3 'OPEN' 0   -1   0.5  1* -0    1*   'Z'  1* /
    'INJECTOR'   2  2 1  1 'OPEN' 1   -1   0.5  1* -6    1*   'X'  1* /
    'INJECTOR'   3  2 1  1 'OPEN' 1   -1   0.5  1* -6    1*   'X'  1* /
    'INJECTOR'   4  2 1  1 'OPEN' 1   -1   0.5  1* -6    1*   'X'  1* /
  /
```

As the well is horizontal, the layer height and the z-permeability are the crucial factors for the connection transmissibility multiplier calculation. Therefore, the Peaceman formula (Eq. 22) must be modified to:

$$r_0 = 0.28 \cdot \frac{\left[\left(\frac{k_z}{k_y}\right)^{1/2} \Delta y^2 + \left(\frac{k_y}{k_z}\right)^{1/2} \Delta z^2\right]^{1/2}}{\left(\frac{k_z}{k_y}\right)^{1/4} + \left(\frac{k_y}{k_z}\right)^{1/4}} \quad \text{.....(36)}$$

4.5.1 Run 14

For the comparison of an unstimulated well with skin factor zero and a stimulated one with skin factor of s = -6, the connection transmissibility multiplier is calculated and included in the simulation data file.

Input: r_w = 0.25 ft

Δy = 1000 ft

Δz = 20 ft

k_y = 500 mD

k_z = 320 mD

Pressure equivalent radius calculation (Eq.36):

$$r_0 = 0.28 \frac{\left[\left(\frac{320}{500}\right)^{1/2} 1000^2 + \left(\frac{500}{320}\right)^{1/2} 20^2\right]^{1/2}}{\left(\frac{320}{500}\right)^{1/4} + \left(\frac{500}{320}\right)^{1/4}} = 124.483\, ft$$

Multiplier calculation (Eq.35):

$$\frac{Twj(s=-6)}{Twj(s=0)} = \frac{\ln\left(\frac{124.483}{0.25}\right)}{\ln\left(\frac{124.483}{0.25}\right) + (-6)} = 29.5085$$

4.5.2 Run 15

As before, the stimulated well with a skin factor of s = -6 is compared to a damaged well with a skin factor of s = +5. The therefore calculated multiplier is inserted in the simulation data file.

Multiplier calculation:

$$\frac{Twj(s=-6)}{Twj(s=0)} = \frac{\ln\left(\frac{124.483}{0.25}\right)+5}{\ln\left(\frac{124.483}{0.25}\right)+(-6)} = 53.2656$$

4.5.3 Result

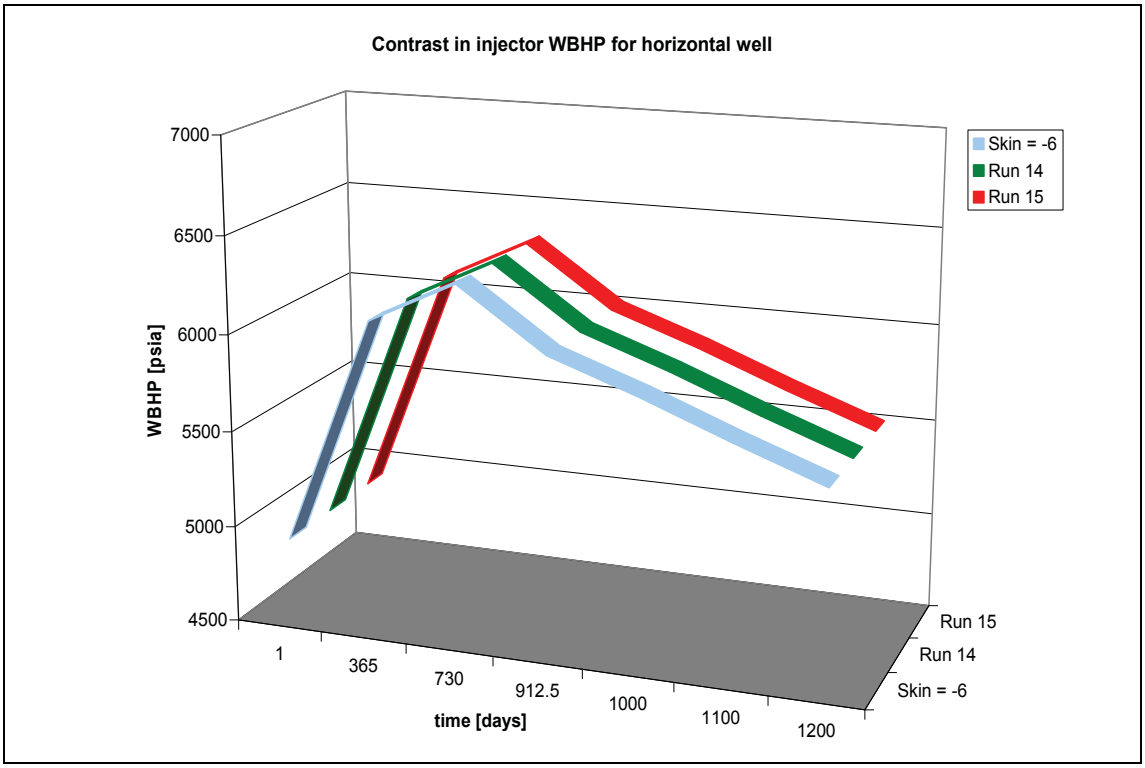

Figure 23: Contrast in injector WBHP for horizontal well

The visual outcome of the connection transmissibility multiplier is still the same as for the stimulated well with a skin factor of s = -6 (Fig. 23). However, Table 5 shows that there is a small difference in the last decimal places, both in the multiplier for the unstimulated and the damaged well. This difference is not only noticeable in the injector well bottomhole pressure, but also e.g. in the field pressure (Table 6). For practical purposes, these differences are negligible.

TIME [days]	Skin = -6 WBHP [psia] INJECTOR	Run 14 WPIMULT = 29.5085 WBHP [psia] INJECTOR	Run 15 WPIMULT = 53.2656 WBHP [psia] INJECTOR
0	4783.102	4783.102	4783.102
1	4917.659	4917.269	4917.263
365	6099.81	6099.774	6099.771
730	6323.332	6323.256	6323.244
912.5	6011.871	6011.79	6011.792
1000	5853.355	5853.275	5853.281
1100	5677.186	5677.107	5677.116
1200	5512.249	5512.175	5512.183

Table 5: Contrast in injector WBHP for horizontal well

TIME [days]	Skin = -6 FPR [psia]	Run 14 WPIMULT = 29.5085 FPR [psia]	Run 15 WPIMULT = 53.2656 FPR [psia]
0	4793.5	4793.5	4793.5
1	4797.306	4797.306	4797.306
365	5785.3	5785.304	5785.303
730	6059.486	6059.438	6059.435
912.5	5737.288	5737.242	5737.253
1000	5585.653	5585.61	5585.626
1100	5419.619	5419.581	5419.599
1200	5264.503	5264.469	5264.488

Table 6: Contrast in field pressure for horizontal well

5 Conclusion

Modeling hydraulically fractured wells in a flow simulation model is limited by a maximum negative skin factor a simulator can handle. This skin factor depends on the geometry and permeability of the grid blocks containing the injection well. If the negative skin factor exceeds a maximum, then the simulation runs into convergence problems or will terminate the simulation run.

In an analytical experiment a formula is derived, which allows a fast approximation of the permissible skin factor of a well that can be used in a simulation. As the permeability is not considered in the derived formula (Eq. 19), it is only applicable in isotropic formations. With the Peaceman formula (Eq. 22) and the calculation of the effective wellbore radius (Eq.12), a very accurate estimation method is presented, which allows the forecast of the permissible negative skin factor also in anisotropic formations. As long as the effective wellbore radius, r_{weff}, is less than the pressure equivalent radius, r_0, the simulation runs without problems. At the point the effective radius exceeds the equivalent radius, the simulation stops. Moreover, the concept of the pressure equivalent radius can be modified for horizontal wells with variable permeabilities in x-, y- and z-direction.

There are cases in the industry, where users would like to run simulations with hydraulically fractured wells which exceed the limiting skin factor. Three different multipliers are developed for these cases and tested to improve the simulation. These multipliers are included in the simulation file instead of a negative skin factor. Primarily, the influence of the multipliers in vertical wells is checked.

The productivity index multiplier (Eq. 24) turns out to be an unsatisfactory method to go beyond the permissible skin factor in a simulation. The multiplier is not influencing reservoir or grid block properties like field pressure, production rates and water cut. In contrast, the difference in the injector well bottomhole pressure due to the utilization of a multiplier is significant.

Also the transmissibility multiplier (Eq. 32) delivers no satisfactory solution. The implementation of such a multiplier influences besides the well bottomhole pressure also all other properties of the simulation. Thus it is not possible to run a correct simulation without implementing the high negative skin factor.

The most promising multiplier is the connection transmissibility factor (Eq. 35). The integration of this multiplier in a simulation run with a skin factor of zero has no influence on properties of other grid blocks. It coincides with the injector well bottomhole pressure of the simulation with a negative skin factor. In several simulation runs the application of the connection transmissibility multiplier is tested for altered geometries, permeabilities and for a well penetrating more than one layer of a vertical well. Additionally, three different skin factor cases are investigated: an injection well with a skin factor of s = -6, a well with an included multiplier and an original skin factor of zero, and a well with a multiplier and an original skin factor of s = +5. In all cases the injector well bottomhole pressure is the same.

In a second step, the application of the connection transmissibility multiplier in a horizontal well is tested. For the utilization of the Peaceman formula in horizontal wells the influence of the boundary conditions has to be considered carefully. Due to the large elongation of the grid blocks in x- and y-direction, the influence of boundary conditions on a vertical well can be neglected. Contrary, the layers in the z-direction are usually thin compared to the x- and y-direction. Hence, in horizontal wells the boundary conditions may affect the simulation result. On this account the application of the connection transmissibility multiplier is also influenced by boundary conditions.

It can be concluded, that the connection transmissibility multiplier is a powerful tool to evade the use of a high negative skin factor in a reservoir simulation. Although the application of this multiplier requires an accurate knowledge of the geometry and permeability of the grid blocks, it is less time- and cost intensive than the creation of a new simulation model.

6 Nomenclature

Latin

A	cross-sectional flow area
B_o	oil formation volume factor
c	unit conversion factor
C_f	fracture conductivity
d	grid block diagonal
g	acceleration due to gravity
G	shear modulus
h	pay thickness or height
H	depth
k	absolute permeability
k_r	relative permeability
p	pressure
p_e	external pressure
p_{wf}	bottomhole flowing pressure
PI	productivity index
q	production- or injection rate
r_0	pressure equivalent radius
r_e	external or drainage radius
r_w	wellbore radius
r_{weff}	effective wellbore radius
s	skin factor
T	transmissibility
T_{wj}	connection transmissibility factor
w	width

Greek

α	Biot's poro-elastic constant
Θ	contact angle of segment connecting with the well

λ_r	relative mobility
μ	fluid viscosity
v	Poisson's ratio
ρ_f	density of overlaying formation
σ_{Hmax}	maximum horizontal stress
σ_{Hmin}	minimum horizontal stress
$\sigma_{H'}$	effective horizontal stress
σ_{tect}	tectonic stress
σ_v	vertical stress
$\sigma_{v'}$	effective vertical stress
Δp	pressure differential
Δp_{skin}	pressure differential due to skin
$\Delta x,y,z$	linear distance difference in x-, y-, or z-direction

Subscripts

f	fracture
o	oil
g	gas
s	skin
x	in x-direction
y	in y-direction
z	in z-direction
i	cell i
j	cell j

7 Appendix A

ODEH reservoir model data file [2, 3, 18]:

```
RUNSPEC
TITLE
   ODEH PROBLEM - IMPLICIT OPTION

DIMENS
   10   10    3  /

NONNC

OIL

WATER

GAS

DISGAS

FIELD

EQLDIMS
    1  100   10    1    1 /

TABDIMS
    1    1   16   12    1   12 /

WELLDIMS
    2    1    1    2 /

NUPCOL
    4 /

START
  19 'OCT' 1982  /

NSTACK
   24 /

FMTOUT

FMTIN

UNIFOUT

UNIFIN

DEBUG
 2  0  0  0  0  0  1/
GRID    ================================================================
-------- IN THIS SECTION , THE GEOMETRY OF THE  SIMULATION GRID AND THE
```

```
-------- ROCK PERMEABILITIES AND POROSITIES ARE DEFINED.
------------------------------------------------------------------------
--  THE X AND Y DIRECTION CELL SIZES ( DX, DY ) AND THE POROSITIES ARE
--  CONSTANT THROUGHOUT THE GRID. THESE ARE SET IN THE FIRST 3 LINES
--  AFTER THE EQUALS KEYWORD. THE CELL THICKNESSES ( DZ ) AND
--  PERMEABILITES ARE THEN SET FOR EACH  LAYER. THE CELL TOP DEPTHS
--  ( TOPS ) ARE NEEDED ONLY IN THE TOP LAYER ( THOUGH THEY COULD BE.
--  SET THROUGHOUT THE GRID ). THE SPECIFIED MULTZ VALUES ACT AS
--  MULTIPLIERS ON THE TRANSMISSIBILITIES BETWEEN THE CURRENT LAYER
--  AND THE LAYER BELOW.
--     ARRAY  VALUE     ------- BOX ------
EQUALS
      'DX'    1000      /
      'DY'    1000      /
      'PORO'  0.3       /

      'DZ'    20        1  10  1  10  1  1  /
      'PERMX' 500       /
      'MULTZ' 0.64      /
      'TOPS'  8325      /

      'DZ'    30        1  10  1  10  2  2  /
      'PERMX' 50        /
      'MULTZ' 0.265625  /

      'DZ'    50        1  10  1  10  3  3  /
      'PERMX' 200       /

/       EQUALS IS TERMINATED BY A NULL RECORD

-- THE Y AND Z DIRECTION PERMEABILITIES ARE COPIED FROM PERMX
--    SOURCE  DESTINATION  ------- BOX ------
COPY
      'PERMX'    'PERMY'   1  10  1  10  1  3  /
      'PERMX'    'PERMZ'   /
/
-- OUTPUT OF DX, DY, DZ, PERMX, PERMY, PERMZ, MULTZ, PORO AND TOPS DATA
-- IS REQUESTED, AND OF THE CALCULATED PORE VOLUMES AND X, Y AND Z
-- TRANSMISSIBILITIES
RPTGRID
  1  1  1  1  1  1  0  0  1  1  0  1  1  0  1  1  1 /

PROPS    ================================================================
-------- THE PROPS SECTION DEFINES THE REL. PERMEABILITIES, CAPILLARY
-------- PRESSURES, AND THE PVT PROPERTIES OF THE RESERVOIR FLUIDS
------------------------------------------------------------------------
-- WATER RELATIVE PERMEABILITY AND CAPILLARY PRESSURE ARE TABULATED AS
-- A FUNCTION OF WATER SATURATION.
--
--  SWAT   KRW   PCOW
SWFN

    0.12  0       0
    1.0   0.00001 0  /

-- SIMILARLY FOR GAS
--
--  SGAS   KRG   PCOG
SGFN
```

```
    0     0       0
    0.02  0       0
    0.05  0.005   0
    0.12  0.025   0
    0.2   0.075   0
    0.25  0.125   0
    0.3   0.19    0
    0.4   0.41    0
    0.45  0.6     0
    0.5   0.72    0
    0.6   0.87    0
    0.7   0.94    0
    0.85  0.98    0
    1.0   1.0     0
/

-- OIL RELATIVE PERMEABILITY IS TABULATED AGAINST OIL SATURATION
-- FOR OIL-WATER AND OIL-GAS-CONNATE WATER CASES
--
--  SOIL     KROW     KROG
SOF3

    0        0        0
    0.18     0        0
    0.28     0.0001   0.0001
    0.38     0.001    0.001
    0.43     0.01     0.01
    0.48     0.021    0.021
    0.58     0.09     0.09
    0.63     0.2      0.2
    0.68     0.35     0.35
    0.76     0.7      0.7
    0.83     0.98     0.98
    0.86     0.997    0.997
    0.879    1        1
    0.88     1        1    /

-- PVT PROPERTIES OF WATER
--
--    REF. PRES. REF. FVF  COMPRESSIBILITY  REF VISCOSITY  VISCOSIBILITY
PVTW
       4014.7     1.029        3.13D-6           0.31            0 /

-- ROCK COMPRESSIBILITY
--
--    REF. PRES   COMPRESSIBILITY
ROCK
        14.7          3.0D-6          /

-- SURFACE DENSITIES OF RESERVOIR FLUIDS
--
--        OIL   WATER   GAS
DENSITY
         49.1   64.79  0.06054  /

-- PVT PROPERTIES OF DRY GAS (NO VAPOURISED OIL)
-- WE WOULD USE PVTG TO SPECIFY THE PROPERTIES OF WET GAS
--
```

```
--   PGAS   BGAS   VISGAS
PVDG
     14.7 166.666   0.008
    264.7  12.093   0.0096
    514.7   6.274   0.0112
   1014.7   3.197   0.014
   2014.7   1.614   0.0189
   2514.7   1.294   0.0208
   3014.7   1.080   0.0228
   4014.7   0.811   0.0268
   5014.7   0.649   0.0309
   9014.7   0.386   0.047   /

-- PVT PROPERTIES OF LIVE OIL (WITH DISSOLVED GAS)
-- WE WOULD USE PVDO TO SPECIFY THE PROPERTIES OF DEAD OIL
--
-- FOR EACH VALUE OF RS THE SATURATION PRESSURE, FVF AND VISCOSITY
-- ARE SPECIFIED. FOR RS=1.27 AND 1.618, THE FVF AND VISCOSITY OF
-- UNDERSATURATED OIL ARE DEFINED AS A FUNCTION OF PRESSURE. DATA
-- FOR UNDERSATURATED OIL MAY BE SUPPLIED FOR ANY RS, BUT MUST BE
-- SUPPLIED FOR THE HIGHEST RS (1.618).
--
--   RS      POIL  FVFO  VISO
PVTO
    0.001    14.7 1.062  1.04    /
    0.0905  264.7 1.15   0.975   /
    0.18    514.7 1.207  0.91    /
    0.371  1014.7 1.295  0.83    /
    0.636  2014.7 1.435  0.695   /
    0.775  2514.7 1.5    0.641   /
    0.93   3014.7 1.565  0.594   /
    1.270  4014.7 1.695  0.51
           5014.7 1.671  0.549
           9014.7 1.579  0.74    /
    1.618  5014.7 1.827  0.449
           9014.7 1.726  0.605   /
/

-- OUTPUT CONTROLS FOR PROPS DATA
-- ACTIVATED FOR SOF3, SWFN, SGFN, PVTW, PVDG, DENSITY AND ROCK KEYWORDS
RPTPROPS
1  1  1  0  1  1  1  1  /

SOLUTION ============================================================
-------- THE SOLUTION SECTION DEFINES THE INITIAL STATE OF THE SOLUTION
-------- VARIABLES (PHASE PRESSURES, SATURATIONS AND GAS-OIL RATIOS)
------------------------------------------------------------------------
-- DATA FOR INITIALISING FLUIDS TO POTENTIAL EQUILIBRIUM
--
--    DATUM  DATUM   OWC    OWC    GOC    GOC    RSVD   RVVD   SOLN
--    DEPTH  PRESS  DEPTH   PCOW  DEPTH   PCOG  TABLE  TABLE   METH
EQUIL
       8400   4800   8500    0     8200    0      1      0       0  /

-- VARIATION OF INITIAL RS WITH DEPTH
--
--    DEPTH    RS
RSVD
       8200  1.270
```

```
       8500  1.270  /

-- OUTPUT CONTROLS (SWITCH ON OUTPUT OF INITIAL GRID BLOCK PRESSURES)
RPTSOL
   1  11*0  /

SUMMARY  =====================================================================
-------- THIS SECTION SPECIFIES DATA TO BE WRITTEN TO THE SUMMARY FILES
-------- AND WHICH MAY LATER BE USED WITH THE ECLIPSE GRAPHICS PACKAGE
------------------------------------------------------------------------------

--REQUEST PRINTED OUTPUT OF SUMMARY FILE DATA

RUNSUM
EXCEL
-- Field Data
FOPR
FOPT
FWPR
FWPT
FLPR
FLPT
FGPR
FGIR
FGPT
FGOR
FWCT
FWIR
FWIT
FPR
FOIP


-- Group Data
GOPR
/
GOPT
/
GWPR
/
GWPT
/
GLPR
/
GLPT
/
GGPR
/
GGPT
/
GGOR
/
GWCT
/
GWIR
/
GWIT
/
-- Well Data
```

```
WOPR
/
WOPT
/
WWPR
/
WWPT
/
WGPR
/
WGPT
/
WLPR
/
WLPT
/
WWCT
/
WGOR
/
WWIR
/
WWIT
/
WBHP
/
WTHP
/
-- WELL GAS-OIL RATIO FOR PRODUCER
WGOR
'PRODUCER'
/

-- WELL BOTTOM-HOLE PRESSURE

WBHP
'PRODUCER'
/

-- GAS AND OIL SATURATIONS IN INJECTION AND PRODUCTION CELL
BGSAT
10 10 3
1  1  1
/

BOSAT
10 10 3
1  1  1
/

-- PRESSURE IN INJECTION AND PRODUCTION CELL
BPR
10 10 3
1  1  1
/


SCHEDULE ================================================================
-------- THE SCHEDULE SECTION DEFINES THE OPERATIONS TO BE SIMULATED
```

```
-----------------------------------------------------------------------
-- CONTROLS ON OUTPUT AT EACH REPORT TIME
RPTSCHED                                              FIELD   10:29 13 JUN 85
   1   1   1   1   1   0   0   0   1   0   0   2   0   1   2   0   0
   0   0   0   0   0   0   0   0   0   0   0   0   0   0   0   0   0
   0   0   0   0   0   0   0   0   0   0   0   0   0   0   0   0   /
RPTRST
 3 0 1 0 0 2 /

-- SET 'NO RESOLUTION' OPTION
DRSDT
      0  /

-- SET INITIAL TIME STEP TO 1 DAY AND MAXIMUM TO 6 MONTHS
TUNING
/
/
/

-- WELL SPECIFICATION DATA
--
--     WELL   GROUP LOCATION  BHP   PI
--     NAME   NAME    I  J   DEPTH DEFN
WELSPECS
    'PRODUCER' 'G'   10 10    8400 'OIL'  /
    'INJECTOR' 'G'    1  1    8335 'GAS'  /
/

-- COMPLETION SPECIFICATION DATA
--
--     WELL     -LOCATION- OPEN/ SAT CONN  WELL KH SKIN D-Factor DIR Ro

--     NAME     I  J K1 K2 SHUT  TAB FACT  DIAM
COMPDAT
    'PRODUCER'  10 10 3  3 'OPEN' 0   -1   0.5  1* -0    1*   'Z'  1* /
    'INJECTOR'   1  1 1  1 'OPEN' 1   -1   0.5  1* -6    1*   'Z'  1* /
  /

-- PRODUCTION WELL CONTROLS
--
--      WELL     OPEN/  CNTL   OIL  WATER   GAS  LIQU   RES   BHP
--      NAME     SHUT   MODE  RATE   RATE  RATE  RATE  RATE
WCONPROD
     'PRODUCER' 'OPEN' 'ORAT' 20000  4*                     1000 /
  /

-- INJECTION WELL CONTROLS
--
--      WELL     INJ   OPEN/  CNTL    FLOW
--      NAME    TYPE   SHUT   MODE    RATE
WCONINJE
     'INJECTOR' 'GAS' 'OPEN' 'RATE'  100000  /
  /

TSTEP
 2*365 182.5  87.5 100.0 100.0
  /

END     ============================================================
```

8 References

1. Economides, M.J., and Nolte, Kenneth G., *Reservoir Stimulation*. 3 ed. 2000, Texas: John Wiley & Sons Ltd.

2. Schlumberger, *Eclipse Reference Manual*, in *Simulation Software Manuals 2007.2*. 2007, Schlumberger.

3. Schlumberger, *Eclipse Technical Description*, in *Simulation Software Manuals 2007.2*. 2007, Schlumberger.

4. BYRON JACKSON Inc., *Applied Engineered Stimulation*. 1970, California: Byron Jackson Inc.

5. Economides, M.J., Hill, A. Daniel, and Ehlig- Economides, Christine, *Hydraulic Fracturing for Well Stimulation*, in *Petroleum Production Systems*. 1994, Prentice Hall, PTR: New Jersey.

6. Economides, M.J., Watters, Larry T., and Sunn-Norman, Shari, *Petroleum Well Construction*. 1998: John Wiley & Sons.

7. Guo, B., Lyons, W., and Ghalambor, A., *Hydraulic Fracturing*, in *Petroleum Production Engineering-A computer-assisted approach*
2007, Elsevier Science & Technology Books: Lafayette.

8. Holditch, S.A., *Hydraulic Fracturing*, in *Petroleum Engineering Handbook-Production Operations Engineering*, J.D. Clegg, Editor. 2007, Society of Petroleum Engineers: Texas.

9. Howard, G.C., and Fast, C.R., *Hydraulic Fracturing*. Monograph ed. T.H.L.D. Series. 1970, New York/Dallas: Society of Petroleum Engineers of AIME.

10. Ruthammer, G., Univ.-Prof. Dipl.-Ing. Dr.mont. , *Lecture notes to Petroleum Production 2*: University of Leoben.

11. Dake, L.P., *Fundamentals of Reservoir Engineering*. 1978, Amsterdam: Elsevier Scientific Publishing Company.

12. Lee, J., *Fluid Flow through permeable media*, in *Petroleum Engineering Handbook- Reservoir Engineering and Petrophysics*, E.D. Holstein, Editor. 2007, Society of Petroleum Engineers: Texas.

13. Economides, M.J., Valko, Peter, and Oligney, Ron, *Unified fracture design: bridging the gap between theory and practice*. 2002: Orsa Press.

14. Hegre, T.M., *Hydraulically Fractured Horizontal Well Stimulation*, in *European 3-D Reservoir Modelling Conference*. 1996: Stavanger, Norway.

15. Sadrpanah, H., Charles, T., and Fulton, J., *Explicit Simulation of Multiple Hydraulic Fractures in Horizontal Wells*, in *SPE Europec/EAGE Annual Conference and Exhibition*. 2006: Vienna, Austria.

16. Settari, A., and Cleary, Michael P., *Three-Dimesional Simulation of Hydraulic Fracturing.* Journal of Petroleum Technology, 1984.

17. Shaoul, J.R., Behr, A., and Mtchdlishvili, G., *Developing a Tool for 3D Reservoir Simulation of Hydraulically Fractured Wells*, in *International Petroleum Technology Conference*. 2005: Doha, Qatar.

18. Odeh, A.S., *Comparison of Solutions to a Three-Dimensional Black-Oil Reservoir Simulation Problem.* Journal of Petroleum Technology, 1981: p. 13-25.

19. Peaceman, D.W., *Interpretation of Well-Block Pressures in Numerical Reservoir Simulation.* SPE Journal, 1978(SPE 6893-PA).

20. Peaceman, D.W., *Interpretation of Well-Block Pressures in Numerical Reservoir Simulation with Nonsquare Grid Blocks and Anisotropic Permeability.* SPE Journal, 1983(SPE 10528).